UNIVERSITY OF BIRMINGHAM

EXPLORING AND EXPLOITING THE MOLECULAR FUNCTION OF ENDOSIALIN (CD248): A CLINICAL BIOMARKER IN INFLAMMATION AND CANCER

by

MR CALLUM POYSER

A thesis submitted to the
University of Birmingham
for the degree of
MASTER OF PHILOSOPHY (MPhil)

Rheumatology Research Group
School of Immunity and Infection
College of Medical and Dental Sciences
University of Birmingham

Supervisor: Professor Christopher Buckley
Co-supervisor: Professor Benjamin Willcox

June 2014

ABSTRACT

Endosialin (CD248) is a novel stromal cell surface receptor that has shown to play a role in both cancer and inflammation. Little is known about CD248's structure, function and mechanism of action.

Deletion mutants of CD248 were generated by overlapping fusion PCR, which were then stably-transfected into MG63 cells, detected by immunofluorescence staining and flow cytometry, and analysed using a growth curve assay. A *Drosophila* S2 cell expression system was used to produce recombinant CD248 protein. Hanging drop crystallisation technique was used to generate protein crystals. Western blotting was used to determine the phosphorylation state of MAPK ERK1/2 in mouse osteoblasts, post-induction with platelet-derived growth factor BB (PDGF-BB).

Crystallisation screening of recombinant CD248 c-type lectin domain (CTLD) and ectodomain generated potential protein crystals for future x-ray crystallographic analysis. Growth curve analysis of CD248 cell surface-expressing MG63 cells demonstrated that the EGF repeat domain may be a key region of CD248 responsible for controlling the proliferation of MG63 cells. Primary osteoblasts from CD248-/- mice exhibited no response to stimulation with PDGF-BB, due to aberrant PDGF signal transduction in CD248-/- mice. This work provides a stepping stone to study and achieve a better understanding of CD248 structure, function and mechanism of action.

ACKNOWLEDGEMENTS

I am grateful to my supervisors Professor Chris Buckley and Professor Benjamin Willcox not only for giving me the opportunity to work on this project in the first place, but for giving constant support throughout and after.

I would like to thank Dr Amy Naylor for help with experimental design, Dr Fiyaz Mohammed for help with Protein crystallography, Mr Mahboob Salim for help with DNA cloning, as well as Miss Sarah Nichols for help and use of the PEF facility.

TABLE OF CONTENTS

LIST OF FIGURES

LIST OF TABLES

Chapter 1

INTRODUCTION

CHAPTER 1 - INTRODUCTION

1.1 Background

1.1.1 Cancer

Cancer therapy has seen great improvements over the past few decades due mainly to recent advances in the areas of molecular medicine, proteomics, genomics and translational research. Progress in cancer genetics has also made it possible to identify genetic patterns that can be used in cancer diagnosis and prognosis. Despite this, cancer still remains the leading cause of death in developed countries accounting for 13% of all deaths each year.

The development of a carcinoma is due to the accumulation of somatic mutations in the epithelial cell layer, however, the subsequent behaviour of a cancer cell is then regulated greatly by the surrounding microenvironment (Bhowmick et al. 2004). The stroma consists of a complex mixture of different cell types such as fibroblasts, lymphocytes, epithelial and endothelial cells along with extracellular matrix components. Molecular cross-talk between cancer cells and the stromal compartment can lead to an abnormal and activated phenotype, function and subsequent tumour progression. For example, it has been long recognised that tumours can induce a modified stroma through activated fibroblast populations, increased extracellular matrix protein expression, angiogenesis and increased lymphocyte populations. For this reason, this unique interplay between the tumour and its microenvironment has been a recent target of therapeutic strategies.

Of particular interest are fibroblasts which have been shown to be the most abundant cell type within the tumour stroma of many cancers, most notably breast and pancreatic cancer (Kalluri and Zeisberg 2006, Pietras and Ostman 2010). Not only do they actively define the structure of the stroma via the synthesis and remodelling of the extracellular matrix components (Gabbiani et al. 1971), but they also play a sentinel role in the immune system by conditioning the cellular and cytokine environment. Cancer-associated fibroblasts (CAFs) have been shown to induce the proliferation and growth of cancer by the overproduction of multiple factors including; extracellular matrix components, cytokines, chemokine's, growth factors, prostanoids (PGE^2), all of which affect cancer and immune cell behaviour (Bromwick et al. 2004). Despite their importance, fibroblast biology has lagged behind research into other cell types; due to its plastic and phenotypic and functional nature, as well as a distinct lack of selective markers for monitoring and isolating such cells.

Cancer growth depends heavily on the formation of new blood vessels to meet metabolic and nutritional needs. For this reason, pericyte's are another stromal cell type of interest for therapy. Pericyte's are endothelial associated mural-derived cells that play an essential role in angiogenesis in terms of; stabilizing newly formed endothelial tubes, vascular splitting, sprouting, endothelial cell proliferation, migration and elongation (Franco et al. 2011). Recent studies have looked at the interactions between endothelial cells and pericyte's which highlights the importance of targeting the stroma as a whole. These two cell types have a mutual relationship; whereby each other's survival and proliferation is the result of bi-directional physical and chemical signalling. For example, pericyte's have been shown to promote endothelial cell survival through the

induction of vascular endothelial growth factor-A (VEGF-A) and Bcl-W expression (Franco et al. 2011). (Bergers et al. 2003) have also shown that endothelial derived platelet derived growth factor (PDGF) induces VEGF expression in pericyte's. Hence, targeting the stromal interactions that support malignant angiogenesis is of great interest for therapy.

1.1.2 Inflammation

Inflammatory disorders such as rheumatoid arthritis (RA) also represents a big problem that affects more than 2.9 million people in Europe alone (Duroux-Richard et al. 2011). RA is the most common inflammatory joint disorder characterised by synovial hyperplasia, ultimately leading to pain, inflammation, as well as bone and cartilage destruction if left untreated. Some of the most successful methods of combating such diseases include early diagnosis and improved therapeutic treatments. The functional parallels between cancer and inflammation have been known about since 1863, when Virchow reported that the origin of cancer derived from sites of ''lymphoreticular infiltrate''. At the cellular level, both conditions are associated with the deposition of new extracellular matrix components and the activation of stromal cells, including fibroblasts, leukocytes and endothelial cells.

Inflammatory diseases such as rheumatoid arthritis are typically characterised by an invasive and joint destructive synovia that exhibits hyperplasia, angiogenesis and inflammatory cell infiltrate leading to the development of lymphoid aggregate structures. Tissue resident stromal (TRS) cells are known to contribute to the progression and persistence of inflammation, via the increased production of pro-

inflammatory cytokines, matrix-degrading enzymes, growth factors, enhanced lymphocyte recruitment and reduced lymphocyte apoptosis. More specifically, TRS cells are able to determine the type and duration of leucocyte infiltration during acute inflammation, and are subsequently able to regulate the withdrawal of such survival signals and leucocyte apoptosis.

Synovial fibroblasts have been shown to be an important stromal cell type in the progression of joint destruction and inflammation, and in the context of rheumatoid arthritis (RA), provide a good example of how stromal cells contribute to the persistence of chronic inflammation. Evidence suggests that RA synovial fibroblasts exert this effect through the altered production of survival signals such as type -1 interferon (IFN-1) (Pilling et al. 1999) and the secretion of chemokine's leading to the accumulation of lymphocyte populations within the synovial joint (Buckley et al. 2000). Activated synovial fibroblasts also secrete proinflammatory growth factors such as VEGF and placental growth factor (PIGF) that increase angiogenesis, synovial hyperplasia, leukocyte recruitment and inflammation (Yoo et al. 2008, Szekanecz et al. 2010). Closely-associated pericyte's are also thought to be involved in the development of arthritis and inflammation. These cell types have been shown to interact with the synovial stroma and in turn regulate the release of a variety of joint-damaging factors; PDGF, VEGF and transforming growth factor beta (TGFβ), (Franco et al. 2011).

1.1.2.2 Bone development (osteogenesis)

Osteogenesis is a dynamic process governed by two types of specialised cells; osteoblasts (involved in bone formation) and osteoclasts (involved in bone resorption). During normal bone development, immature osteoblast cells are recruited to the site of bone formation (Maes et al. 2010), whereby they are kept in an immature state via PDGF signalling (Sanchez-Fernandez et al. 2008). Once they have undergone differentiation, mature osteoblasts become non-proliferative and upregulate type 1 collagen (Liu et al. 1997). In certain inflammatory disorders such as RA this process is perturbed, and more specifically is characterised by inflammation-induced focal bone loss. Within the inflammatory microenvironment, osteoclast differentiation is enhanced and osteoblast-mediated bone formation is inhibited leading to bone erosion and overall net weight loss. A number of studies have reported a lack of mature osteoblasts at the sites of focal bone erosion in RA (Gravallese et al. 1998) and murine inflammatory arthritis (Zwerina et al. 2006) and have linked perturbed osteoblast function to site-specific bone loss (Walsh et al. 2009).

1.1.3 Endosialin (CD248)

1.1.3.1 Introduction

In an effort to better understand the biology and role of stromal cells in cancer and inflammation, cell surface marker proteins have been identified that are differentially expressed between normal and diseased tissue. A study in 1992 that screened for monoclonal antibodies that specifically recognised proteins on reactive fibroblasts, successfully identified Endosialin (CD248) as an antigen that was selectively expressed in vascular endothelial cells of malignant tumours (Rettig et al. 1992). Later in 2000, a

serial gene expression analysis (SAGE) study that involved comparing gene transcript levels on endothelial cells derived from blood vessels of normal and malignant colorectal tissues, also highlighted CD248 as the most upregulated in terms of gene expression (St Croix et al. 2000). Both these studies subsequently sparked a growing interest into the possibility of CD248 as a target for anti-angiogenesis therapies.

CD248 has been mapped to chromosome 11 (11q13-qter) by serologic analysis of a panel of rodent-human somatic cell hybrids (Rettig et al. 1992), whereas the corresponding mouse gene has been mapped to chromosome 9 (Opavsky et al. 2001). In 2001, the human CD248 gene was further characterised through molecular cloning of human CD248 cDNA (Christian et al. 2001). This study revealed that the CD248 gene consists of a 2274bp open reading frame that codes for a type I transmembrane glycoprotein with a molecular mass of around 80.9 kDa. Interestingly, the gene was found to be intronless and sequence alignment with its mammalian homologues has revealed a high level of sequence identity and conservation across vertebrates (Opavsky et al. 2001).

The transcription initiation site is situated 17 bps upstream of the start codon (ATG). Opavsky et al. (2010) have demonstrated that CD248 gene transcription is upregulated in response to high cell density *in vitro.* This is thought to be mediated via the binding of transcription factor SP1 to the promoter region. In addition, a more recent study has reported an upregulation of CD248 gene expression during hypoxia (Ohradanova et al. 2008). More specifically, they showed that Hypoxia-inducible factor 2 (HIF-2) activates

the endosialin promoter both directly and indirectly, through binding to the hypoxia-responsive element (HRE) or through Ets-1, respectively.

1.1.3.2 Family members

CD248 belongs to a family of C-type lectin-like transmembrane proteins implicated in tissue remodelling and repair. The word lectin is derived from the latin *legere*, meaning 'to select' and is used to define proteins that have the ability to bind soluble carbohydrates or moiety's as part of glycoproteins. The term CTL is used to distinguish a group of calcium-dependent lectin's, from the calcium-independent forms. The C-type lectin (CTL) superfamily is a large well studied group of metazoan proteins with diverse functions such as adhesion and glycoprotein synthesis. The classification of such proteins was first outlined in a review published by Drickamer (1989) whereby he grouped CTLD-containing proteins into seven groups (I to VII) based on sequence analysis and domain organisation. Since then, the classification has been revised with the addition of seven new groups (Drickamer 1999, Drickamer and Fadden 2002).

The Thrombomodulin family (Group XIV) consists of four-related proteins; endosialin (CD248), thrombomodulin (TBM), complement receptor protein (CD93) and C-type lectin domain family member 14A (Clec14A) (Figure 1A). All members are characterised by a CTLD protruding from the cell surface in addition to a sushi domain, epidermal growth factor repeats (EGF) and a highly glycosylated mucin-like region. Despite variation in overall amino acid identity between such family members, they maintain a high level of conservation in the globular domains and are all in some way involved in vascular biology.

Thrombomodulin is a well characterised molecule with a variety of known roles, including cell adhesion, in tumourigenesis and in the anticoagulant pathway (Hanly et al. 2005), (Weiler and Isermann 2003), all mediated by different domains. For example, Wang et al (2000) have previously shown that EGF domains 5 and 6 are responsible for thrombin binding in the anticoagulant pathway. Whereas, another study has demonstrated that the CTLD of thrombomodulin plays an important role in preventing leukocytes from binding to the endothelium which in turn causes inflammation (Conway et al. 2002).

CD93 was first identified by its role in activating phagocytosis in human monocytes via its interaction with complement factor C1q (Nepomuceno et al. 1999). CD93 is thought to function as a cell adhesion molecule (Dean et al. 2000). One such study that supports this hypothesis, reported the binding of the CTLD of CD93 to the endothelial cells (McGreal and Gasque 2002).

Clec14A is the most recently discovered, and for that reason is the least studied member of the Thrombomodulin family. Two very recent studies have described Clec14A's role in angiogenesis as a tumour endothelial marker (TEM), more specifically functioning in migration, tube formation and endothelial cell-cell adhesion via a CTLD-mediated interaction (Rho et al. 2011), (Mura et al. 2012).

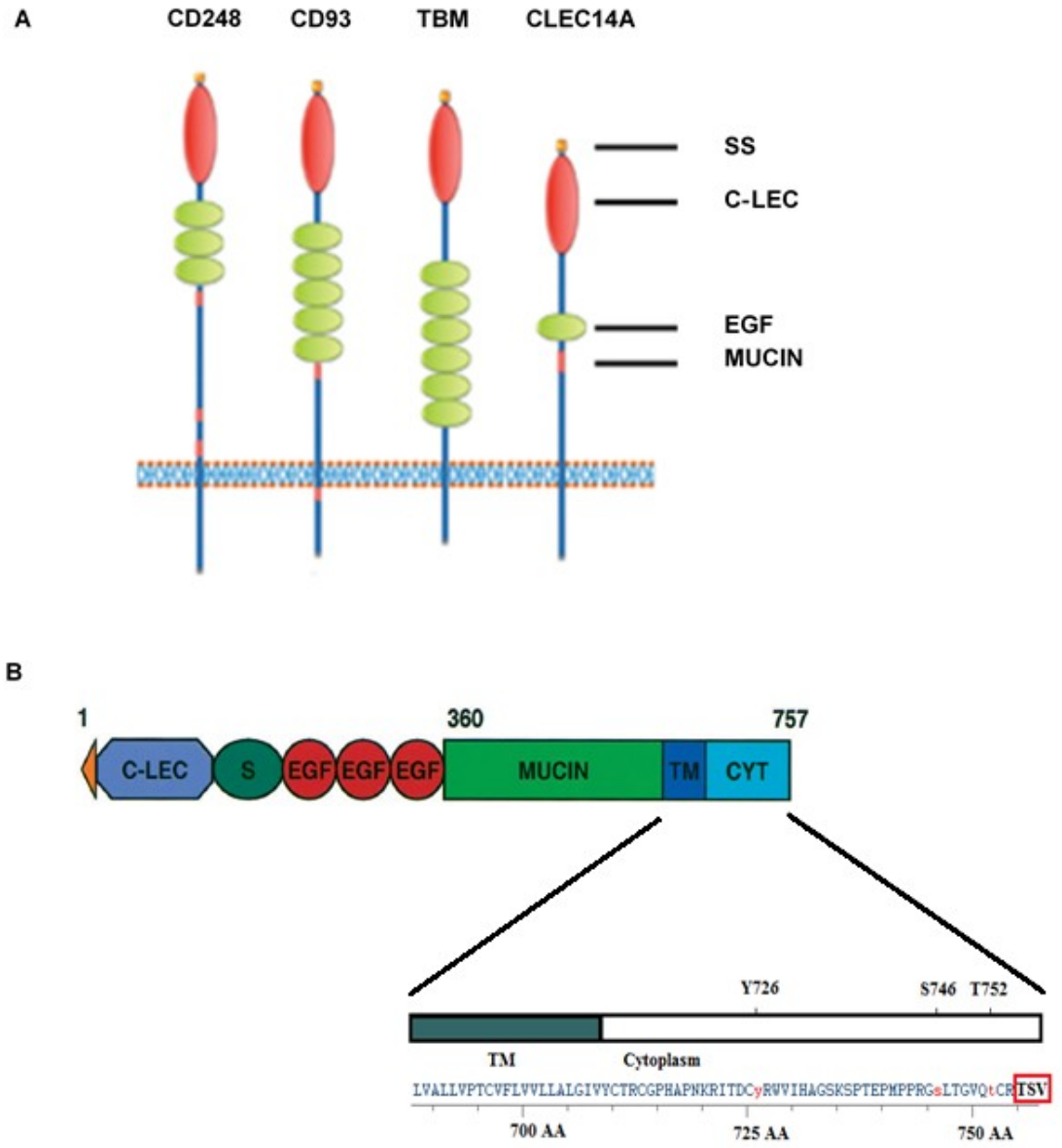

Figure 1. CD248 is a member of the C-type lectin family 14. (A) Schematic diagram comparing CD248 with other members of the C-type lectin family 14. (Taken and adapted from Mura et al 2012). (**B**) Schematic diagram of CD248-specific domain organisation: The N-terminal signal leader peptide (SS, orange), the C-type lectin domain (C-LEC), the Sushi domain (S) and three EGF repeats (EGF) followed by the mucin-like region (MUCIN), the transmembrane section (TM) and the short cytoplasmic tail (CYT) (Modified from (Christian et al. 2001).

1.1.3.3 Structure

CD248 is composed of several functional domains, none of which have yet been linked to any molecular functions. At the extreme N-terminus is a predicted short 20 amino acid (AA) leader peptide thought to assist translocation into the endoplasmic reticulum (Christian et al. 2001). Immediately downstream is a C-type calcium-dependant lectin (CTLD, 157 AA long). This domain has no known function and despite its classification, prediction software indicates that CD248 does not retain the sequences required for Ca^{2}+ dependant ligand binding and has not been proven yet. Downstream of the CTLD is a sushi or complement control protein (CCP, 57 AA long). Multiple sushi domains are commonly found in proteins involved in regulation of the complement system, such as complement receptor type 1 (CR1/CD35) and factor H (Nangaku 1998). CD248 also contains three epidermal growth factor (EGF) repeats (156 AA) and a mucin-like region (269 AA) (Fig 1) of which is modified extensively by o-linked glycosylation (Christian et al 2001), a single transmembrane (48 AA) and a short cytoplasmic tail (51 AA), (Christian et al. 2001). The intracellular tail contains three potential phosphorylation sites and a PDZ-binding motif (4 conserved residues) at the extreme c terminus (according to PhophoSite). The latter have for a long time been recognised as protein-binding motifs that bind to intracellular proteins that contain 80-90 AA long PDZ domains and help organize small local protein complexes for signal transduction. Therefore, the PDZ-binding motif of CD248 may contribute to intracellular signalling pathways that lead to disease states.

1.1.3.4 Ligand interactions

Few studies have looked at how expression is linked to its effects in cancer and inflammation. However, some *in vitro* studies suggest that the ectodomain of CD248 may interact with particular extracellular matrix proteins including collagen 1, 4 and fibronectin (MacFadyen et al. 2005). More recently, another group have given evidence for an interaction with a tumour derived ligand Mac-2 binding protein (Mac-2 BP), commonly linked to metastasis, which was shown to result in decreased tumour cell-myofibroblast adhesion (Becker et al. 2008). It is unlikely that the ectodomain binds sugars in a calcium-dependant manner due to the lack of conserved key amino acids in the CTLD, whereas the sushi, EGF and mucin-regions have all been shown to have the potential for calcium-independent binding in other receptors. Perhaps more interestingly, recently published data generated by the Claire Isackes lab have shown based on pericyte-EC co-culture assays that CD248-Fc binds to an EC-specific matrix protein (Simonavicius et al. 2012). In terms of intracellular ligand interactions, none have been found thus far. However, the cytoplasmic tail is bound to be important as this structure has been shown to be vital in RA and tumour growth mouse models (Maia et al. 2010, Maia et al. 2011).

1.1.3.5 Expression

CD248 exhibits a very restricted cellular expression profile. Originally there was some debate as to whether CD248 was also expressed by endothelial cells or closely-associated pericyte's, after being defined as a tumour endothelial marker (TEM), (St Croix et al. 2000). MacFadyen et al. (2005) later demonstrated that CD248 was in fact expressed by endothelial-associated pericyte's, not the endothelial cells themselves

using co-localisation with the pericyte marker NG2. MacFadyen et al. (2005) also reported the fibroblast-restricted distribution of CD248 by generating a panel of monoclonal antibodies towards isolated human fibroblasts. A recent study demonstrated that CD248 is predominantly expressed on perivascular and fibroblast-like synovial cells in the synovium from patients with psoriatric arthritis (PsA) and RA (Maia et al. 2010). CD248 is also expressed on mesenchymal stem cells (MSCs) from the bone marrow (Bagley et al. 2009). MSCs are highly plastic cell type in nature, and have the ability to differentiate into adipocytes (fat), chondrocytes (muscle) or osteoblasts (bone). In fact, *In silico* mining of gene expression data. Su et al (2004) has shown that CD248 is highly expressed on osteoblasts. In addition, CD248 expression has recently been described on naïve $CD248^{+}$ T lymphocytes (Hardie et al. 2011).

CD248 exhibits an interesting expression profile at the organ and tissue level. CD248 is expressed throughout a wide variety of tissues and organs during embryonic development not limited to the; heart, liver, brain, spleen, and neuroectoderm (Rupp et al. 2006, Lax et al. 2007). However, CD248 expression gets progressively less post-natally until absent on normal adult tissue. A variety of studies have confirmed high expression in a variety of different types of cancer, including sarcomas (Brady et al. 2004), (MacFadyen et al. 2005), gliomas (Rettig et al. 1992), sarcomas (Huber et al. 2006) and xenografts (Carson-Walter et al. 2009), specifically restricted to the stromal and perivascular cells.

A more recent, less studied observation is the upregulation of CD248 on inflamed tissue. Maia et al. (2010) have recently reported high CD248 expression in synovial

tissue from RA and PsA patients, compared to healthy tissue. Even more recently Smith et al. (2011) demonstrated that CD248 is also upregulated in human chronic kidney disease (CKD) which was linked to known determinants of renal progression.

1.1.3.6 Signalling

The signalling mechanisms by which CD248 mediates its functions are controversial and largely unknown. The first study that provided evidence for the possible involvement of PDGF signalling was performed by (Christian et al. 2008), whereby they showed that CD248 knock-down in human fibroblasts leads to reduced migration in a PDGF-BB-dependant manner. Since then, a more recent study has described the mechanism by which CD248 regulates pericyte proliferation (Tomkowicz et al. 2010). It was reported that CD248 acts by the phosphorylation of the PDGF receptor, activation of MAP kinase ERK 1/2 and subsequent upregulation of c-fos transcription factor. The exact location at which CD248 intersects PDGF downstream signalling is still to be determined. However, this recent finding suggests that CD248 may recruit Src/PI-3 and c-fos pathways to exert its effect. The small cytoplasmic tail has no known kinase function but potential phosphorylation sites may interact with intracellular molecules in a direct or indirect-fashion.

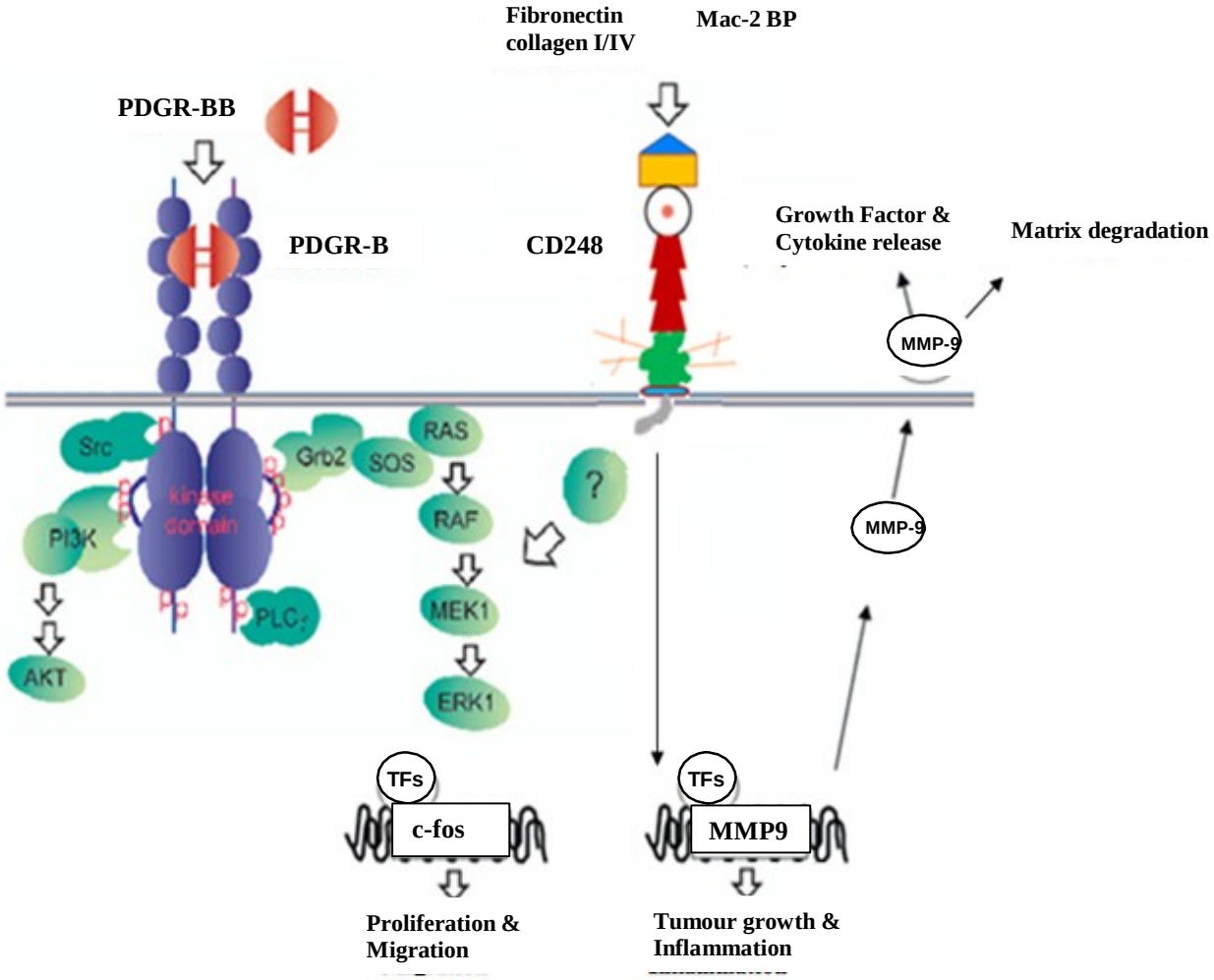

Figure 2. **Schematic representation of CD248-dependant signalling pathways and their proposed downstream functional effects**. CD248 is required for PDG-signalling downstream of the PDGFR-B receptor: PDGF-B, secreted by activated endothelial or cancer cells, phosphorylates the PDGF Receptor, effectively upregulating downstream pathways involving Src/PI-3/ERK kinase, leading to the increased expression of c-*fos* which promotes proliferation. In addition, extracellular matrix proteins (Fibronectin and Collagen I/IV) bind to the CD248 ectodomain leading to increased cellular migration via the upregulation of matric matrix matelleoprotease 9 (MMP9) and subsequent matrix degradation. An additional metastasis-

related ligand Mac-2 binding protein has also been described (taken and adapted from (Demoulin 2010)).

1.1.4 CD248 in Cancer

The functional significance of CD248 upregulation on stromal fibroblasts and pericyte's in cancer is still largely unknown. But, functional studies in mice and in humans have provided evidence for an active role in tumour growth, invasiveness, metastasis and neovessel formation in a variety of cancer types; including breast, colon, renal, pancreatic, lung and sarcomas. For example, *In vivo* studies in mice show that CD248 is required for the progression of certain tumours; abdominal tumours that have been implanted into CD248-deficient mice exhibit a reduction in growth and metastasis as well as vasculature maturation defects (Figure 3).

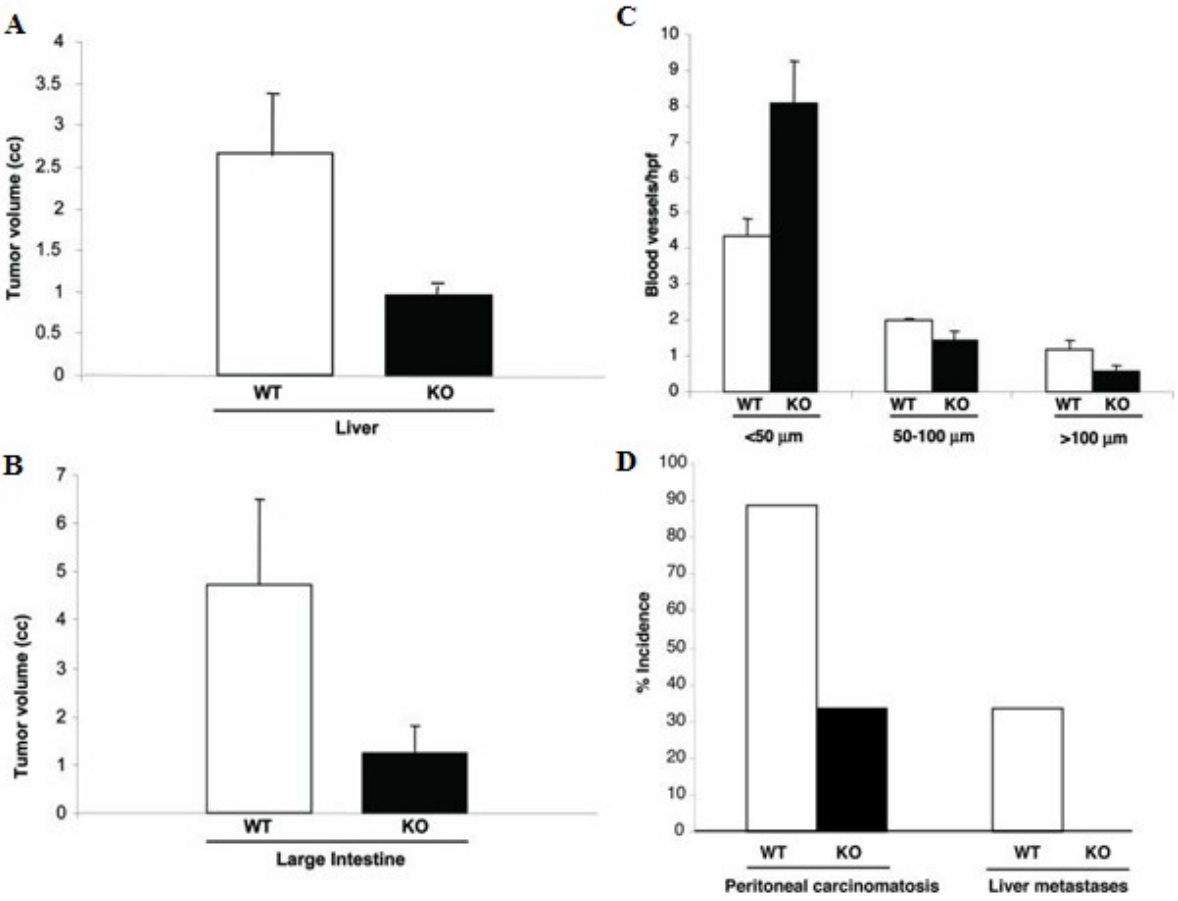

Figure 3. The Effects of CD248 in Cancer. (**A**) and (**B**) Growth of tumours in immunocompetent mice. (**C**) Angiogenesis in abdominal tumors showing vessel number and size (**D**) Incidence of peritoneal carcinomatosis and liver metastasis (taken and adapted from (Nanda et al. 2006)).

Recent studies have highlighted a number of functions at the cellular level. It has been reported that cells that overexpress CD248 exhibit increased cellular migration and cell-cell adhesion (Tomkowicz et al. 2007). Lax et al. (2007) have also shown that the

migration levels and proliferative capacity of mouse embryonic fibroblasts (MEF) derived from CD248-deficient mice are significantly lower than WT controls (Figure 4).

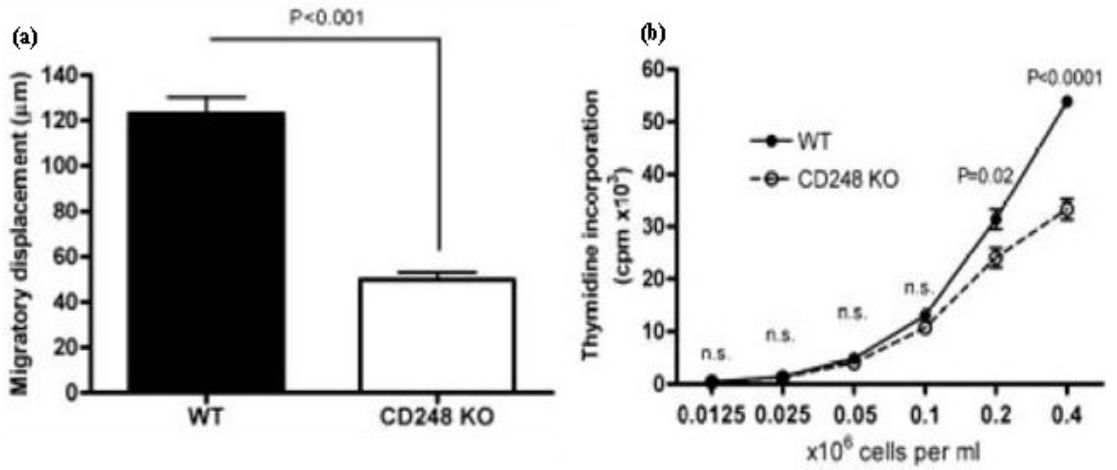

Figure 4. The Effect of CD248 on cellular migration and proliferation. (**A**) Migration levels of MEF derived from CD248 KO mice is considerably lower compared to WT control as assayed using a Dunn chamber. (**B**) Proliferative capacity of MEF derived from CD248 KO mice is significantly reduced relative to WT controls based on 3H uptake (taken and adapted from (Lax et al. 2010)).

Other studies have reported similar functional effects, most notably cellular proliferation (Christian et al. 2008) migration and tube formation (Bagley et al. 2008a, Bagley et al. 2008b).

It is not clear how these molecular functions result in their cellular effects, but as mentioned earlier, the finding that CD248 can bind to the extracellular matrix proteins (collagen 1, 4 and fibronectin), thereby upregulating matrix metalleoproteinase 9

(MMP9) that in turn mediates cell adhesion and cellular migration represents a possible explanation for CD248's role in increased tumour growth and metastasis (via increased growth factor and cytokine release from the extracellular matrix, Figure 2). In addition, the expression, function and effects of CD248 suggest a role in early angiogenesis (Bagley et al. 2008b) and vessel maturation. The fact that CD248 expression is regulated by hypoxia also indicates a role in the formation and reorganization of the tumour stroma as well as blood vessels in areas of hypoxia and increased growth (Christian et al. 2008).

1.1.5 CD248 in Inflammation

The first indication that CD248 may also play a role in inflammation and the immune system was the reported upregulation of CD248 expression in stromal fibroblasts derived from the rheumatoid joint (MacFadyen et al. 2005) as well as on a specific subset of stromal cells involved in lymphoid tissue remodelling and repair, post infection (Lax et al. 2007). CD248 involvement has since been extended to other inflammatory disorders such as chronic kidney disease (CKD) and inflammatory bowel disease (IBD). The former study, reported the up regulation of CD248-expressing stromal cells and the correlation with known determinants of renal progression and disease outcome (Smith et al. 2011). The molecular mechanism by which CD248 causes its effects is unknown but is likely to be a result of increased cellular proliferation, migration, cytokine and chemokine factor release as seen in cancer progression, due to the fact that both disorders are characterised by an activated fibroblast population and mesenchymal cell involvement. In fact, more recent studies have shown that mice deficient in CD248 develop less severe arthritis and display characteristics such as

reduced synovial hyperplasia, leukocyte infiltration and cytokine levels (Maia et al. 2010).

1.1.6 CD248 is a Clinical Biomarker and Therapeutic Target.

The fact that CD248 is upregulated in inflammation and cancer, in combination with a number of other desirable characteristics makes this receptor a prime candidate for the development of a novel molecular biomarker, for which there is a growing need. From a therapeutic perspective, the current state of knowledge suggests that the interaction between CD248-expressing stromal cells and extracellular matrix components represents a good strategy for inhibiting tumour progression. In addition, the fact that CD248 is a marker for tumour-associated pericyte's makes it an attractive target for anti-angiogenic therapy, and the inhibition of proven fibroblast and pericyte functional characteristics such as proliferation and migration may offer therapeutic benefit, by interfering with the stromal contribution to inflammatory disease. There is currently a drive in the area of designing novel therapies which aim to inhibit CD248 in the form of potent blocking antibodies and small molecule inhibitors. There is an anti-CD248 monoclonal antibody (MORAb-004) currently being developed and is undergoing phase 1 and 2 clinical trials for the treatment of solid tumours (ClinicalTrials.gov identifier: NCT008470544), due to promising preclinical pharmacological results highlighting its usefulness as an anti-cancer drug.

1.2 The Aims

The central theme of this research was to address the structure-function paradigm with the overall aim of investigating the molecular basis of CD248 function. Specifically, the first aim was to generate protein crystals of CD248 CTLD and complete extracellular domain in an effort to generate structural data. The second aim was to identify the growth characteristics of MG63 cells stably transfected with different CD248 mutant constructs in an effort to define key functional domains. The final aim was to provide a molecular mechanism for the observed effect of CD248 in osteoblast function and subsequent bone formation.

CHAPTER 2

MATERIAL AND METHODS

CHAPTER 2 - MATERIAL AND METHODS

2.1 Material

2.1.1 Bacterial strains, cell lines and plasmids

DH5α *E.coli* cells were used as a host for constructing and propagating plasmids, whereas BL21 (DE3) *E.coli* host cells were used as a bacterial expression host. *Drosophila* Schneider 2 (S2) cells for protein production were obtained from Invitrogen (#R690-07). MG63 cells, a human osteosarcoma fibroblast-like cell line for protein expression studies were kindly given to me by Dr Debbie Hardie (Rheumatology Research Group, University of Birmingham).

The mammalian expression vector for the human CD248 cDNA (pcDNA 3.1+) was purchased from Invitrogen. It contained both a c-myc and polyhistidine tag for purification and detection purposes. A Kozak sequence was introduced directly upstream of the start codon to allow the efficient translation of the recombinant protein. CD248 protein-coding regions were amplified from a plasmid previously generated in our group (Lax et al. 2010). For recombinant protein production in the *Drosophila* S2 system, the pMT/BiP/V5-His expression plasmid (Invitrogen) was used which contained a metallothionein promoter (pMt) for heavy metals inducible expression. It also contained a V5 epitope, polyhistidine tag, biotinylation tag and a hygromycin resistance gene.

2.1.2 Primers

Custom-designed primers were purchased from Invitrogen Life Technologies and prepared using TE buffer.

2.1.3 Buffers, solutions and chemicals

Agar plates: Agar poweder was added to LB medium to a final concentration of 1.5% and autoclaved. Solid LB-agar was then melted in a microwave and 100 μg/ml of ampicillin was added, before being poured into petri dishes and stored at 4 ° C.

Agarose: Molecular Biology grade (Sigma-Aldrich #05066).

Ampicillin: Working concentration 100 μg/ml (Sigma #A0166). Stored at -20˚C

Cell Dissociation Buffer: Trypsin/EDTA 10X sterile filtered (Sigma #T4174).

Coomassie Blue stain: 1.25 g Brilliant Blue, 250ml ddH_20, 50ml acetic acid.

Coomassie De-stain: 150ml Methanol, 300ml H_20, and 50ml acetic acid.

Drosophila S2 medium: SF900-SFMII medium (Invitrogen # 12658-019) containing 10% heat inactivated foetal bovine serum (FBS) and hygromycin once transfected.

DNA Ladder: 100bp (Invitrogen #15628-019).

DNA Loading Buffer: 0.25% Bromophenol Blue, 0.25% xylene cyanol, 15% Ficol and ddH_20.

DNA stain: Hoescht stain (Molecular Probes #33258)

Ethidium Bromide: used a t a final concentration of 0.5 μg/ml

dNTPs: prepared 10mM stock DNTP SET - A,C,G,T (GE Healthcare #28-4065-62)

FCS: (Invitrogen #10106-169)

Freezing medium: Working concentration 10% DMSO in 90% FCS (Sigma #D8779).

Fluorescence Activated Cell Sorting (FACs) buffer: 3% BSA in PBS

Geneticin (G418): Working concentration 500 ug/ml (Sigma #A1720). Stored at -20˚C

High Imidizole buffer: 100mm Imidizole 20mM $Na_2PO_4H_20$, 0.5M NaCl pH7. Low Imidizole Buffer: 10mM Imidizole, 20mM $Na_2PO_4H_20$, 0.5M NaCl pH7. Mounting solution: Polyvinyl alcohol with DABCO® antifading gel (Sigma #10981). MG63 Growth Medium: DMEM, 10% FCS.

Ni-NTA magnetic Agarose Beads (Qiagen #30210).

Non-enzymatic dissociation buffer: StemPro Accutase (Invitrogen #A11105-01).

Optimem Reduced Serum Medium: (Invitrogen #2017)

Paraformaldehyde (4%): Paraformaldehyde powder dissolved in PBS (Sigma #158127)

PBS: Tablet dissolved in ddH_20 (1 per 100ml), (Sigma #P4417).

Refolding Buffer: 100 mM Tris pH 8.0, 400 mM L-arginine, 2 mM EDTA, 0.5 mM oxidized glutathione, 5 mM reduced glutathione and 0.1 mM PMSF with a final pH of 8.3.

Restriction enzymes: All purchased from NEB.

SDS Running Buffer: Prepared from 10X Tris-Glycine-SDS ready-made buffer (Sigma #T7777).

SyPro orange dye: (Invitrogen # 6650)

TBE: 89mM Tris Base, 89mM Boric acid, 2mM EDTA.

TBS-T: 100 mM Tris pH 7.5, 150 mM NaCl, 0.1 % Tween-20

Triton-X-100: Sigma #T9284.

T4 DNA ligase (5X): (NEB MO202S).

Western Blot Transfer Buffer: 25 mM Tris pH 8.0, 192 mM glycine, 10 % methanol, ddH_20.

Velocity DNA Polymerase: (Bioline #21098).

2.1.4 Antibodies and kits

Table 1. Antibodies

Name	Host Species	Source	# No.
anti-human CD248 B1/35.1	Mouse	Isacke Lab	-
anti-mouse p44/42 MPAK	Rabbit	eBioscience	4695
anti-mouse phospho-p44/42 MAPK	Rabbit	eBioscience	9101
anti-His (c-terminal)	Mouse	Invitrogen	R930-CUS
anti-mouse IgG HRP	Rabbit	Invitrogen	61-6520
anti-mouse IgG Cy5	Goat	Invitrogen	A10524
anti-mouse IgG FITC	Rabbit	Invitrogen	616511

Dynabeads® M-280 Sheep Anti-Mouse IgG (Invitrogen #112-01D)

ECL Plus Western Blotting Detection Reagent (GE Healthcare #RPN2132)

Lipofectamine 2000 Transfection Reagent (Invitrogen #11668)

Plasmid Mini Kit (QIAGEN #27104)

Plasmid Maxi Kit (QIAGEN #12163)

Nitrocellulose membrane (Amersham #RPN203G)

QIAquick Gel Extraction Kit (QIAGEN #280704)

X ray Film: Kodak X-OMAT (Sigma #F1149)

2.2 Methods

2.2.1 Molecular Biology Techniques

2.2.1.1 Polymerase Chain Reaction (PCR) and Overlapping PCR mutagenesis

All PCR reactions were carried out using Velocity DNA polymerase according to the manufacturer's instructions. Full length cloning was conducted using the following reaction mixture; 20 pmol of each primer, 0.5 μg template DNA, 250 μM dNTPs, 5 x Hi-Fi Buffer, 3% DMSO and 1 unit of Velocity enzyme, made up to total volume of 50 μL with PCR-grade water. The following standard cycling conditions were used; 1 cycle at 98 ° C for 2 min, followed by 25 cycles at 98 ° C for 30 secs, 50-68 ° C for 30 secs, and 72 ° C for 1 min 30 secs, and 1 final cycle at 72 ° C for 10 min.

Overlapping PCR mutagenesis was conducted using a modified version of the protocol above. Two internal primers were designed for each desired domain deletion, one sense and the other antisense which contained a 30 bp overlapping sequence with one another, respectively (Table 2). Two separate PCR reactions were then carried out. PCR 1 used the 5' end sense primer which introduced ATG start codon and EcoRI site, in combination with the reverse antisense primer. PCR 2 used the Forward internal primer with the 3' antisense primer which introduced a TGA stop codon and XbaI site. This effectively generated two overlapping PCR products, which when verified (by agarose gel electrophoresis), purified (QIAgen kit) and subjected to a third round of PCR to anneal them together generated DNA coding the entire CD248 domain deletion insert. This was done in a 2-step manner; 1uL (20ng) of PCR1 and 2 were mixed together in combination with Velocity DNA polymerase, buffer, dNTPs, DMSO and water. One cycle of denaturation, annealing and extension was performed. The second step

involved (CD248 Full length 5' and 3' F and R) adding primers to a final volume of 50 μL, and running a standard velocity PCR program. The final PCR fusion products were then analysed by agarose gel electrophoresis to verify they were of the expected size, digested with EcoRI and XbaI and ligated into the pcDNA 3.1 expression vector in a similar way to the wild-type construct.

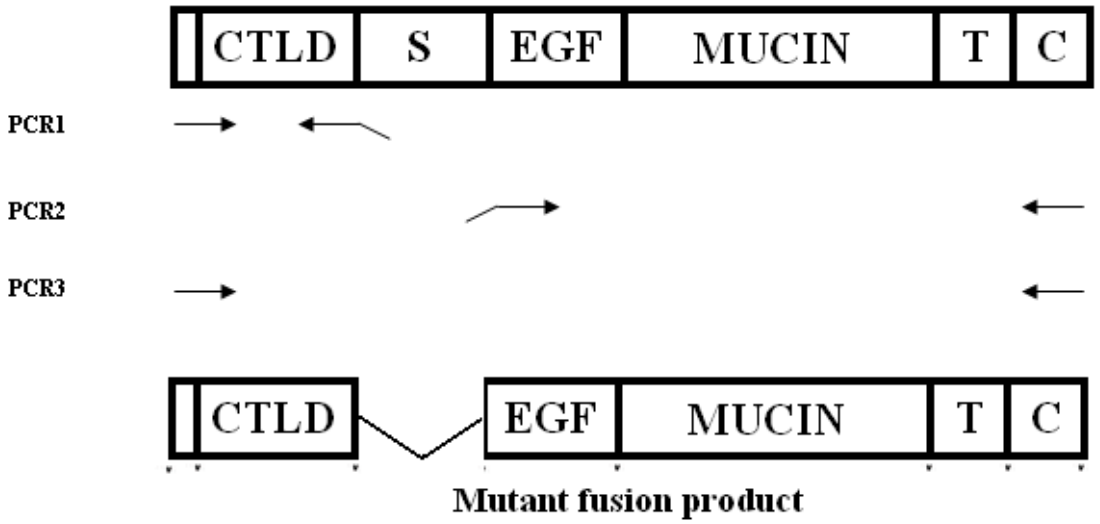

Figure 5. Overlapping PCR mutagenesis of CD248. The example shown above is for the generation of CD248_Δ sushi. The 1st PCR reaction used a sense primer that was complementary to the N-terminus with a 5' overhanging region, in combination with an antisense primer that was complementary to the beginning of the sushi domain. The 2nd PCR reaction used a sense primer that was complementary to the start of the EGF repeat domain and an antisense primer that was complementary to the C-terminus end of CD248. The 3rd PCR reaction used the overlapping PCR products from reaction 1 and 2 and the forward and reverse CD248 primers to amplify a fragment containing the full CD248 sequence minus the desired domain deletion.

Table 2. Overlapping PCR mutagenesis oligonucleotide primers

	PCR 1		PCR2		PCR3	
Gene Insert	**Forward Primer** (5' to 3')	**Reverse Primer** (5' to 3')	**Forward Primer** (5' to 3')	**Reverse Primer** (5' to 3')	**Forward Primer** (5' to 3')	**Reverse Primer** (5' to 3')
WT CD248	---------- -	----------	----------	---------- -	GCGAATTCGCC ACCATGCTGCTG CGCCTGTTGCTG	GCTCTAGATCA CACGCTGGTTCT GCAGGT
CD248_Δ CTLD	GCGAATTCGCC ACCATGCTGCTG CGCCTGTTGCTG	GCAGGCGGCAC GGGGCTCAGCA GC	CCCTGGGCTGCTGAG CCCCGTGCCGCCTGC CAGTTTGGCTTCGAG GGCGCCTGC	GCTCTAGATCA CACGCTGGTTCT GCAGGT	GCGAATTCGCC ACCATGCTGCTG CGCCTGTTGCTG	GCTCTAGATCA CACGCTGGTTCT GCAGGT
CD248_Δ sushi	GCGAATTCGCC ACCATGCTGCTG CGCCTGTTGCTG	CTCGAAGCCAA ACTGGCACAGG TA	GACGGCTTACCTGTG CCAGTTTGGCTTCGA GACTGGCTGCAGCCT GACAACGGG	GCTCTAGATCA CACGCTGGTTCT GCAGGT	GCGAATTCGCC ACCATGCTGCTG CGCCTGTTGCTG	GCTCTAGATCA CACGCTGGTTCT GCAGGT
CD248_Δ EGF	GCGAATTCGCC ACCATGCTGCTG CGCCTGTTGCTG	CACACAGCGGT GCGGATCATCC TC	CCAGCGGAGGATGA TCCGCACCGCTGTGT GCCTGCAGGGGCCA TGGGTGCCCAG	GCTCTAGATCA CACGCTGGTTCT GCAGGT	GCGAATTCGCC ACCATGCTGCTG CGCCTGTTGCTG	GCTCTAGATCA CACGCTGGTTCT GCAGGT
CD248_Δ Muc	GCGAATTCGCC ACCATGCTGCTG CGCCTGTTGCTG	CGTCCAGCCAC CGTTGAAGGCC TTC	GCCTGGAAGGCCTTC AACGGTGGCTGGAC GACAGCCCTGGGGG AGGCTGGTCTTG	GCTCTAGATCA CACGCTGGTTCT GCAGGT	GCGAATTCGCC ACCATGCTGCTG CGCCTGTTGCTG	GCTCTAGATCA CACGCTGGTTCT GCAGGT
CD248_Δ CYT	----------	----------	----------	----------	GCGAATTCGCC ACCATGCTGCTG CGCCTGTTGCTG	GCTCTAGATCA CACGCTGGTTCT GCAGGT

2.2.1.2 Agarose gel electrophoresis and gel purification

1% agarose was prepared in Tris-Acetate-EDTA (TAE) buffer, cooled and supplemented with ethidium bromide (0.5 μg/ml) to visualise the DNA. DNA samples were diluted in 5 X loading buffer prior to being loaded, separated at a constant voltage (80 V) and visualised using a UV box. Extraction and purification of DNA was carried using the Gel Extraction Kit (QIAGEN) according to the manufacturer's instructions.

2.2.1.3 Restriction enzyme digestion

10 μg of purified DNA was incubated with 1-2 U of each restriction enzyme, 10 X Buffer, in a final volume of 40 μl at 37 ° C for 1.5-2 hours. The resultant digestion products were analysed and purified as described above.

2.2.1.4 Bacteria transformation

20 μl of competent cells were gently thawed on ice, mixed with 1μl of purified plasmid DNA and incubated on ice for a further 20 minutes, before being heat-shocked for 1 min at 42 ° C. The resultant mixture was then mixed with 250 μl of SOC medium for 1 hour in an orbital shaker at 37 ° C, of which 100 μl was spread onto an LB agar plate (containing 100 μg/ml ampicillin) and left overnight at 37 ° C.

2.2.1.5 Plasmid DNA preparation

An overnight culture (5 ml LB amp derived from a single colony of freshly-transformed *E.coli* DH5 alpha) was harvested and the plasmid DNA was purified using a Miniprep kit according to the manufacturer's instructions. Maxiprep of plasmid DNA was conducted in a similar way using the QIAprep Maxiprep kit.

2.2.1.6 Colony screening

Successful cloning was confirmed by colony PCR or restriction digest analysis prior to DNA sequencing. Colony PCR involved inoculating cells into a 20 µl standard PCR reaction. Test digests were conducted with 10 µl of purified miniprep plasmid DNA. PCR products and digestion products were analysed by agarose gel electrophoresis.

2.2.1.7 DNA Sequencing

Purified DNA samples were sent along with vector-specific primers to and performed by the Functional Genomics and Proteomics unit at the University of Birmingham utilising an ABI 3730 capillary sequencer.

2.2.2 Recombinant protein production

2.2.2.1 E.coli cells

Recombinant protein was expressed as insoluble inclusion bodies in *E.coli* as routinely performed by our laboratory (Garboczi et al. 1992). Briefly, chemically-competent *E.coli* Bl21 (DE3) cells were transformed by standard heat shock method. Single colonies of transformed *E.coli* cells were then grown as starter cultures (LB medium supplemented with 100 µg/ml ampicillin) in an orbital shaker at 37° C before being transferred into 5L flask containing LB medium (supplemented with ampicillin) and induced by the addition of isopropyl β-D-1-thiogalactopyranoside (IPTG). Overexpressed recombinant proteins were then purified and solubilised from inclusion bodies via sonication, homogenisation and dissolved in 8M Urea. The resulting inclusion bodies were analysed by SDS page prior to refolding. Chemical refolding of proteins was performed by the standard Garboczi method (Garboczi et al. 1992).

Briefly, refolding was initiated by pulse-step dilution of approximately 30mg of protein into 500mL refold buffer overnight at 4° C. The refold mixtures were then concentrated down to 10 mL using Amicon centrifugal filtration devices.

2.2.2.2 Drosophila S2 cells

S2 cells were grown at 27° C in T-25/ T-75 flasks in standard *Drosophila* medium, and supplemented with hygromycin once transfected. Cells were generally subcultured every 5 days (1:6), and seeded at a density of 1.2 $x10^6$/ mL. Transfection was performed by standard $CalCl^2$ methods by the in-house technician Sarah Nichols. For large scale expression, S2 transfected cells were first subcultured into 125 mL of selective Schneider medium (500mL flask) supplemented with 0.05% Pluronic F-68 surfactant for 4 days, prior to transfer into a final volume of 250mls in a 1L flask. Once the cells reached a density of ~3-5 x 10^6/ml, protein expression was then induced by the addition of CuSO4. After 3-5 days, the supernatant was collected via two rounds of centrifugation and stored in 0.02% Na Azide at 4° C.

2.2.2.3 SDS-polyacrylamide gel electrophoresis (SDS-PAGE)

Recombinant proteins were separated on a 15% polyacrylamide gel, which was prepared as outlined in the table below (Table 3). The polymerised gel was then placed into the tank and filled with SDS running buffer. Approximately 10 μg of protein was mixed with reducing or non-reducing 5x SDS sample buffer boiled at 95 ° C for 5 minutes and loaded alongside a molecular weight marker. Electrophoresis was performed at 120 V then increased to 180V once through the stacking gel. Gels were

then stained with Coomassie stain for 30-45 minutes with orbital shaking followed by De-stain solution for a further 30-45 minutes.

Table 3. SDS-PAGE gel components for recombinant protein analysis

		15% Separation (ml)	Stacking (ml)
30% Acrylamide		5.0	**0.67**
ddH20		2.3	**2.7**
Tris Buffer	1M; pH 8.8	0.5	/
	1M; pH 6.8	/	**2.5**
10 % SDS		0.1	**0.04**
APS		0.1	**0.04**
TEMED		**0.004**	**0.004**

For electrophoretic separation prior to western blot analysis of cell lysates, cells in 1 well of a 6-well plate were lysed directly in 100 µl of 1x Non-Reducing buffer. The lysates were then centrifuged for 3 min at 100g of which 20 µl of supernatant was loaded per lane (alongside pre-stained marker) of a 12% polyacrylamide gel (Table 4).

Table 4. SDS-PAGE gel components for cell lysate analysis

		12% Separation (ml)	5% Stacking (ml)
30% Acrylamide		6	**1.3**
ddH20		5.25	**6.1**
Tris Buffer	1.5M; pH 8.8	3.75	/
	0.5M; pH 6.8	/	**2.5**
10 % SDS		0.15	**0.2**
APS		0.075	**0.1**
TEMED		**0.003**	**0.002**

2.2.2.4 Western blotting

Following electrophoresis, the separated protein bands were transferred to a 0.45μm PVDG nitrocellulose membrane using a BioRad Trans-well apparatus according to the manufacturer's protocol. The blots were then blocked in 5% skimmed milk in 1 x Tris buffered saline tween (TBST) for 1 hour to block non-specific binding of antibody.

For CD248 detection in *Drosophila* supernatant, the blot was stained with a mouse anti-His antibody (1:500) for 1 hour. The blot was subsequently washed in 3 stages with 1 x TBST before incubation with anti-mouse IgG HRP (1:1000) for 1 hour and 3 further washes. Proteins were visualised using enhanced chemiluminescence (ECL) kit and exposure to x-ray film ranging from 10 secs to 1 min.

For MAPK detection in osteoblast lysates, the blot was stained with anti-mouse p44/42 MPAK or anti-mouse phosphor-p44/42 MAPK primary antibodies (1:2000) overnight at 4° C on a rotating platform and detected with anti-mouse HRP (1:10,000) in a similar manner.

2.2.2.5 Affinity chromatography

1L of supernatant was dialyzed in 10X PBS buffer. The dialyzed supernatant was then transferred to a column pre-loaded with 1ml of Ni-NTA agarose beads overnight at 4° C. The next day the column was washed with 200ml of Low Imidazole-containing buffer to remove non-specifically bound proteins and eluted off the column with 7-8 ml of High Imidazole-containing buffer into 1ml fractions and analyzed by SDS-PAGE.

2.2.2.6 Size-exclusion chromatography (SEC)

SEC was performed using a Sepherose S200 column on an Akta FPLC machine (Amersham Biosciences) in combination with UNICORN software. In the first step 1 litre of appropriate purification buffer was filter-sterilised and washed over the column. The s loop was then washed with 5ml of the same buffer followed by insertion of 7-10ml of pre-filtered protein sample onto the column at a maximum flow rate of 2.5ml/min. The peak corresponding to the molecular weight of the protein was collected and analysed by SDS page. Quantification of protein was performed by measuring the optical density at 280 nm in combination with relevant absorption coefficients.

2.2.2.7 Buffer optimisation

We used the thermofluor method as a high-throughput approach for identifying optimal protein buffer for purification and crystallization. The fluorescence thermal shift assay was performed as described before (Ericcson et al 2006). Each reaction contained protein, SyPro Orange in a 96 well plate. A melting curve program was run on the standard RT-PCR machine with a 1°C temperature increase every 30 seconds up to 100°C. Computer software calculated the first derivative values (amplification plot) from raw fluorescence data to determine Tm (dissociation plot) A change in Tm of > 10°C was deemed as a significant difference that is likely to yield improved protein stability in solution.

2.2.2.8 Crystallisation screening

Preliminary crystallisation screens were set up using the automated Mosquito robot (TTP LabTech), via the hanging drop and sitting drop method. Protein was suspended over wells (96-well format) containing a variety of commercially purchased screens; Wizard I/II, JCSG+, SS, PEG R/X. Conditions yielding potential crystals were then followed up in large scale format, following negative control screens. Hanging and sitting drops were inspected for crystal formation after 3 days and on a weekly basis thereafter.

2.2.4 Cell culture and analysis

2.2.4.1 Culture conditions and passaging of cells

The osteosarcoma MG63 cells were cultivated in complete fibroblast media, in a humidified incubator at 37 ° C with 10% CO_2.

Adherent cells were passaged once 70-80% confluent. This was performed via incubation with trypsin/EDTA solution for 5 minutes, followed by centrifugation at1,000g for 5 min and resuspension in fresh medium with 33% conditioned medium before being seeded into new T75 flasks for continued culture at around $6x10^4$ cells/ml.

2.2.4.2 Storage of cells

Adherent cells from a T75 flask were detached using Trypsin-EDTA, re-suspended in standard fibroblast medium, centrifuged at 1,000g for 5 min and then re-suspended in 3 ml freezing medium before being aliquoted into 1 ml cryo-vials and stored at -80 ° C. Cryo-vials were later transferred into liquid nitrogen for long term storage.

2.2.4.3 Transfection and generation of stably transfected cells

All transfections were carried out using Lipofectamine 2000 reagent and procedure. MG63 Cells were plated at a cell density of 3-5 x 10^5 in a 6-well format in 2 ml of serum-free Optimem. The next day, for each cell of wells to be transfected, 2μg of endotoxin-free plasmid DNA was diluted into 250 μl of Optimem and 6-10 μl. Lipofectamine reagent was diluted into 250 μl of Optimem separately, before being mixed together at room temperature for 20 minutes to form DNA-Lipofectamine complexes. 500 μl of complex mixture was then added to each well in a drop wise manner, followed by incubation at 37 ° C. Stably transfected cells were then selected for 48 hours post transfection using Geneticin selection media (500 μg/ml) for 2-4 weeks making sure to change the media every few days.

2.2.4.4 Positive isolation

Magnetic beads coated with anti-mouse IgG were used to positively select cells of interest. After the Dynabeads were washed with PBS/BSA, harvested cells were labelled with CD248 monoclonal antibody B1/35.1 (IgG1 supernatant) on ice for 20 minutes. In the second step labelled cells were bound with antibodies to magnetic beads by incubating 1ml of cells with 25 μl of Dynabead solution for 20 minutes at 4 ° C. In the final step, the bead-bound cells were isolated using the magnetic separator. The tube was placed into the magnetic separator for 2 minutes, supernatant was removed and the bound cells were washed multiple times to remove any residual unbound cells. Afterwards cells were re-suspended in complete fibroblast medium and seeded into T75 flasks for continuous culture.

2.2.4.5 Immunofluorescence and FACs analysis

Adherent cells were plated at 3-5 x 10^4 cells per well in an 8-well chamber slide and cultured in fibroblast medium overnight. The next day, cells were washed with PBS and fixed with ice cold 3% paraformaldehyde (PFA) for 10 minutes. Cells were then blocked in 1% bovine serum albumin (BSA), PBS solution for 1 hour at room temperature to reduce non-specific antibody binding, before being incubated with the appropriate primary antibody for a further 1 hour. This was followed by 2-3 washes with PBS solution. Cells were labelled with CD248 monoclonal antibodies B1/35.1 (1:3) and detected with incubation with anti-mouse IgG Cy5 (1:10,000) for 1 hour in the dark. After extensive washing in PBS, cells were incubated with the DNA stain (Hoechst) for 5 min and mounted with Dabco solution after brief rinses with PBS. Non-specific binding of antibodies was further controlled for by omitting the primary

antibody. Images were obtained using a LSM 510 confocal microscope (Zeiss, Welwyn Garden City, UK) equipped with a FITC and far-red filters.

For FACs analysis, cells were harvested using a non-enzymatic dissociation buffer, counted and centrifuged at 100g for 5 minutes then re-suspended in FACs buffer at 1-5x10^5 cells/ml. Cell staining was performed in polystyrene round bottomed tubes in a final volume of 30-50 μl/ tube. Single-cell suspensions were incubated with CD248 monoclonal antibody B1/35.1 (1:3) for 30-45 min on ice. Cells were then washed with FACs buffer by centrifugation at 100g for 5 minutes, re-suspended in anti-mouse Ig FITC (1:50) for 30 min on ice in the dark before being washed again, centrifuged and re-suspended in 500 μl of FACs buffer for analysis on a Cyan FACS analyser in conjunction with Summit software. Data were further analyzed using FlowJo Version 7.2 software (TreeStar).

2.2.4.6 Growth curve assay

Cells were seeded in triplicate at a density of 1 x 104 cells per 24-well and cultured in complete fibroblast medium, under normal culturing conditions (37 ° C, 10% CO_2). Cells were then harvested via trypsinization on days 1, 2, 3, 4, 5, 6, 7 and counted using a haemocytometer. The media in the remaining well was replaced with fresh media every 2-3 days.

CHAPTER 3

MUTAGENESIS OF CD248

CHAPTER 3 - MUTAGENESIS OF CD248

3.1 Introduction

As mentioned earlier, CD248 has a known role in tumour growth, metastasis, wound repair and inflammation. Recent evidence suggests that CD248 may cause these effects by increasing the proliferation and migration of CD248-expressing stromal cells. Specifically, mouse embryonic fibroblasts (MEFs) derived from CD248 knockout mice have been reported to exhibit a significantly lower proliferative and migratory capacity compared to wild type MEFs (Lax et al. 2010). Despite such data, it is not yet known which region of the protein is critical for such observations. Therefore, this chapter describes the generation, characterisation and analysis of CD248 mutants in an effort to determine which structural domains may be responsible for these known effects.

3.2 Results

3.2.1 Construction and Transfection of CD248 or its mutants

To construct WT and mutant CD248-containing mammalian expression vectors, the full length cDNA encoding human CD248 was amplified and subcloned into the EcoRI/XbaI sites of pcDNA 3.1^{+} plasmid (Methods section 2.2.1.1) to obtain CD248WT-pcDNA 3.1 construct. The same CD248-containing plasmid was used for overlapping fusion PCR (Methods section 2.2.1.1) whereby specific domains were deleted and given the following names; CD248_Δ CTLD, CD248_Δ sushi, CD248_Δ EGF, CD248_Δ mucin, CD248_Δ cytoplasmic. A schematic representation of the CD248 gene illustrating the domains targeted for PCR amplification and mutagenesis can be seen in Figure 6 alongside the

corresponding products from the individual PCR reactions. The sizes of the products in Figure 6 are consistent with the expected fragment sizes, for example in an effort to generate CD248_Δ CTLD fragment, the 1st PCR reaction produced a ~ 100bp, the second produced a ~1800bp fragment, and the third fusion reaction produced a fragment of 2000bp. The different CD248 mutant inserts were then subcloned into EcoRI/XbaI sites of pcDNA 3.1^{+} plasmid, maxiprepped, and fully sequenced to confirm successful mutagenesis and subsequent cloning (data not shown).

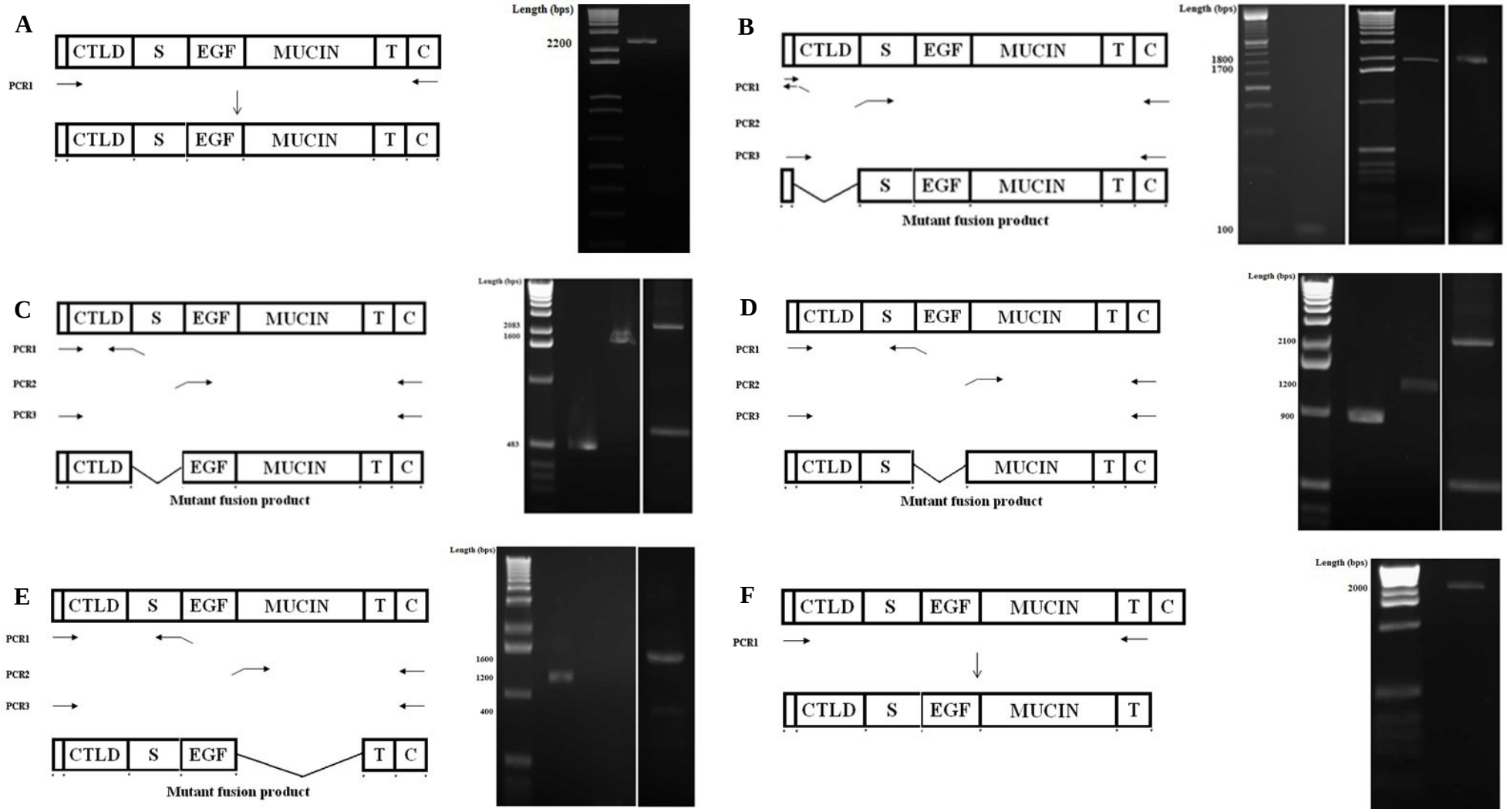

Figure 6. Generation and electrophoretic analysis of WT CD248 and mutant fusion products from overlapping PCR-generated fragments by overlap extension PCR (described in detail in methods section). (**A**) amplification of full length CD248 in a single PCR reaction, (**B**) PCR1 and 2 generated a 100 bp and 1700bp fragments, respectively, which were then fused to make CD248_Δ CTLD of 1800bp fragment, (**C**) PCR1 and 2 generated a 400 bp and 1600bp fragments, respectively which were fused to make CD248_Δ sushi 2kb fragment, (**D**) PCR1 and 2 generated a 900 bp and 1200bp fragments, respectively which were fused to make CD248_Δ EGF 2.1 kb fragment, (**E**) PCR1 and 2 generated a 1200 bp and 400 bp fragments, respectively which were fused to make CD248_Δ mucin 1.6 kb fragment, (**F**) amplification of full length CD248 minus the cytoplasmic tail in a single PCR reaction.

To generate CD248-expressing stable cells, myc-tagged plasmid DNA encoding wild-type or mutant CD248 were individually transfected into MG63 osteosarcoma cells (express no endogenous CD248). All transfections were carried out as described in methods section 2.2.4.3. Stably transfected cells were established 2-4 weeks later following antibiotic selection. Magnetic beads coated with anti-mouse IgG and anti-CD248 B1/35.1 antibody were then used to positively select for CD248-expressing cells as described in methods section 2.2.4.4.

3.2.2 Expression and subcellular localization of CD248 or its mutants in MG63 cells

Resulting stably transfected cells were then fixed in paraformaldehyde (3%) and analysed by immunofluorescence staining for CD248 and correct subcellular localisation. Untransfected MG63 cells were used as CD248-negative Controls.

By confocal microscopy, the B1/35.1 anti-CD248 monoclonal antibody detected exogenous CD248 expressed by the MG63 transfected cells (Figure 8). However, the anti-myc antibody directed to the c-terminal myc tag was unable to detect such CD248 expression. It can be seen from Figure 7 that CD248 is expressed at moderate levels in all of the transfected cells whilst no background staining was seen in the negatively transfected MG63 cells (Figure 7) and no antibody control (data not shown).

The subcellular distribution of CD248 was not consistent across all stably transfected cell populations. The localisation of CD248 in CD248_Δ sushi, CD248_Δ EGF stably-expressing cells appeared to be predominantly cell surface staining, as well as some cytoplasmic staining (Figure 7). Whereas CD248 staining appeared to be predominantly

cytoplasmic with very little cell surface staining in the CD248_WT, CD248_Δ CTLD, CD248_Δ mucin, CD248_Δ cytoplasmic stably-expressing cells (Figure 7). The cytosolic staining was not uniformly spread but exhibited a granular pattern characteristic of that seen with the proteins associated with endoplasmic reticulum or Golgi vesicles.

In addition, the percentage of CD248 cell surface expressing cells were analysed by flow cytometry (Figure 8). The method as outlined in Section 2.2.4.5 used the B1/35.1 anti-CD248 monoclonal antibody in an unconjugated fashion. It can be seen from Figure 9, that the CD248_Δ sushi, CD248_Δ EGF stably-expressing cells exhibited two peaks of fluorescence, populations of cells. In the CD248_Δ sushi cell line, the first peak comprised 58.7% of the cells. The second peak comprised 42.3% of the cells which represented the CD248-positive cell population (Figure 8). Likewise, in the CD248_Δ EGF cell line, the second peak comprised 43.4% CD248-positive cells population (Figure 8). However, the CD248_WT, CD248_Δ CTLD, CD248_Δ mucin, CD248_Δ cytoplasmic cell lines exhibited negligible shifts in fluorescence (Figure 8).

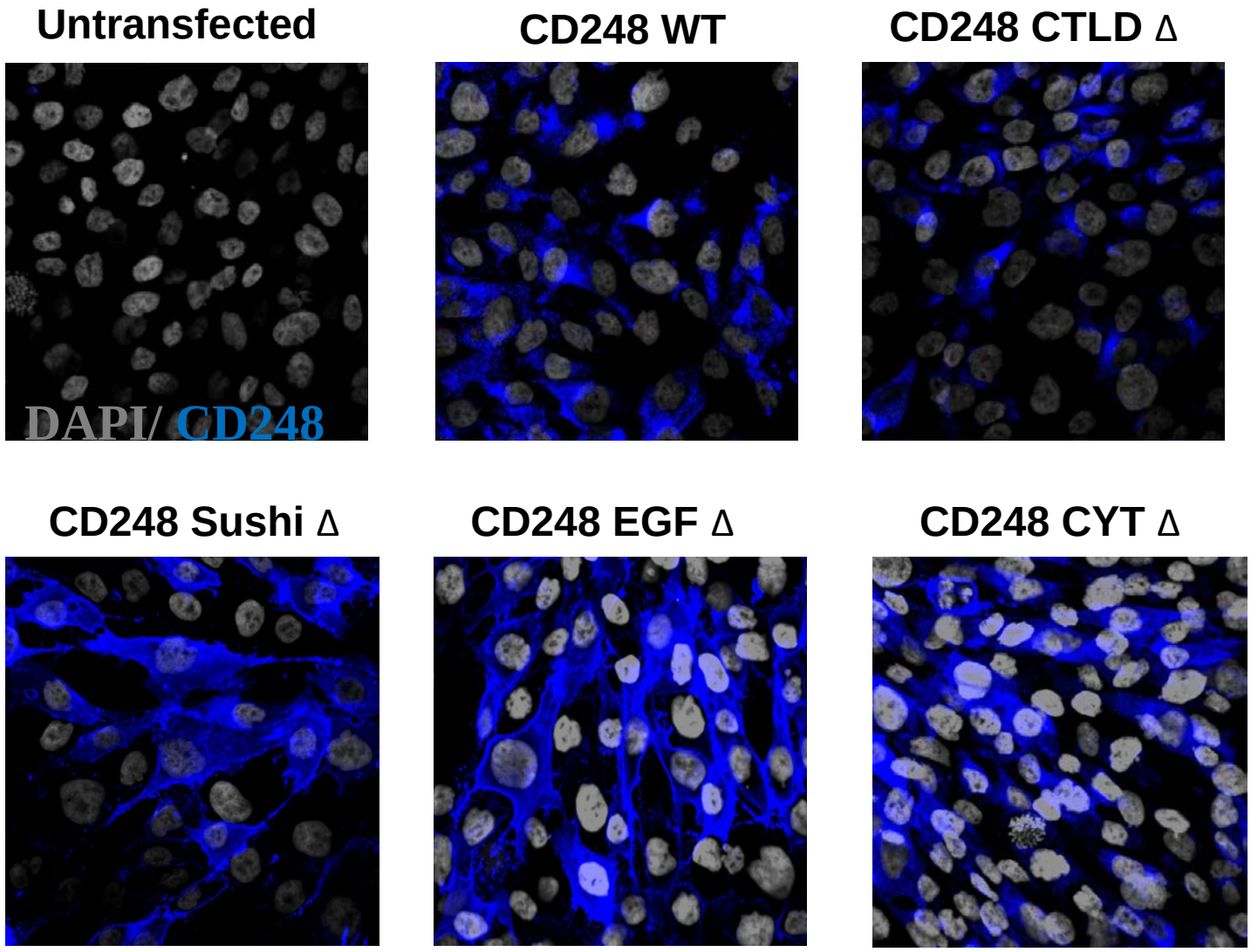

Figure 7. Immunoflourescence analysis of myc-tagged CD248 in stably-transfected MG63 cells. myc-tagged CD248 was transfected into to MG63 cells using the Lipofectamine 2000 (Invitrogen). The cells were fixed with 3% paraformaldehyde 2-4 weeks post transfection following antibiotic selection and stained with B1/35.1 anti-CD248 antibody and detected with anti-mouse IgGCy5 secondary antibody. The nucleus (grey) was stained with Hoechst DNA stain. The cells were observed by confocal microscopy. All images were taken at 25X zoom factor.

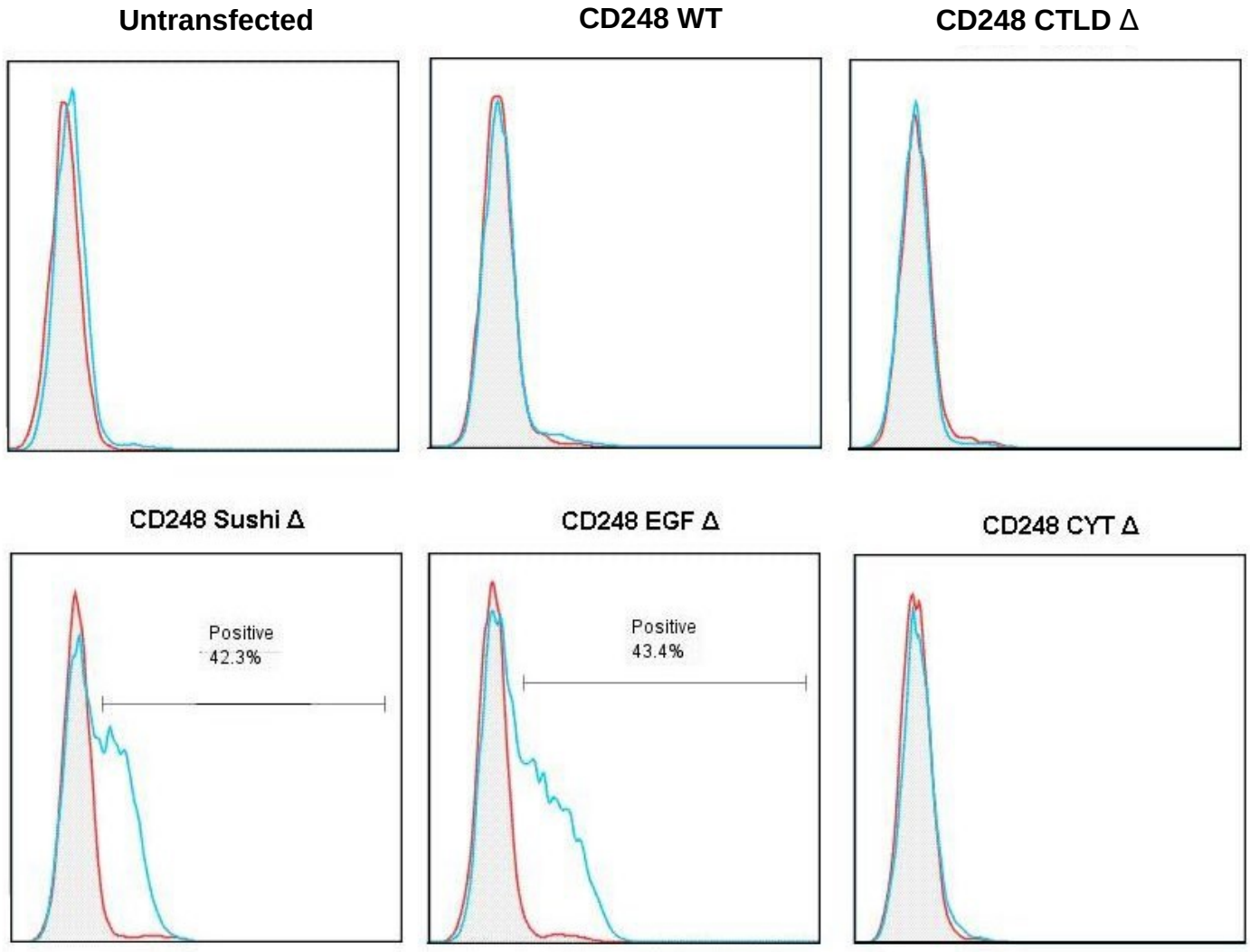

Figure 8. Flow cytometry analysis of myc-tagged CD248 in stably-transfected MG63 cells. myc-tagged CD248 was transfected into to MG63 cells using the Lipofectamine 2000 (Invitrogen). Cells were harvested using a non-enzymatic dissociation buffer 2-4 weeks post transfection following antibiotic selection and stained with B1/35.1 anti-CD248 antibody and detected with anti-mouse IgG FITC secondary antibody. Fluorescence is indicated on the *x*-axis.

3.2.3 Overexpression of CD248_Δ sushi increases the growth rate of MG63 cells

The CD248_Δ sushi, CD248_Δ EGF cell surface-expressing MG63 cells were then used in subsequent functional assays. Growth curve analysis was performed to determine the possible role of either of the sushi or EGF domains in the proliferation of MG63 cells. To determine the growth ability of each cell line, each cell population was analysed for cell number every day for a week, post-seeding into 24-well plates (Methods section 2.2.4.6) and subsequent growth curves were drawn (Figure 9).

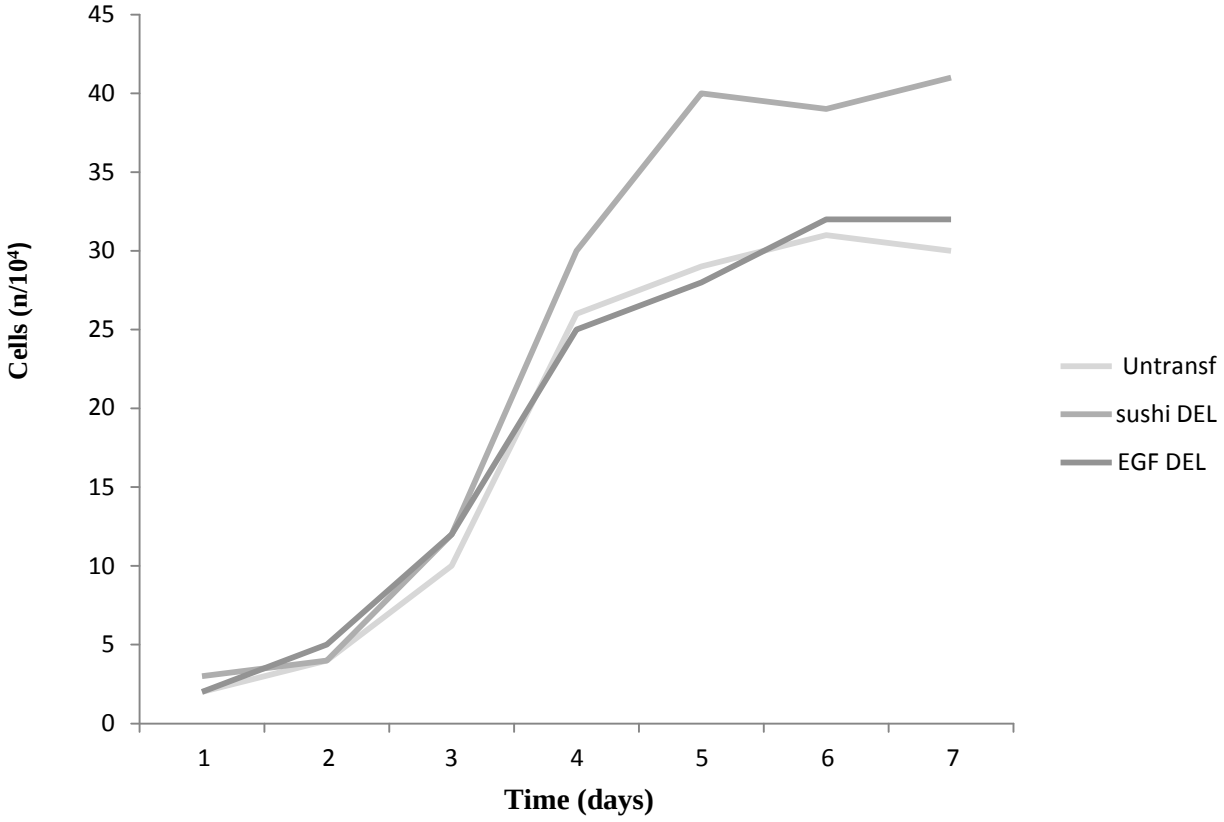

Figure 9. Growth curves of untransfected, CD248_Δ sushi, CD248_Δ EGF-expressing MG63 cells. Each cell population was cultured in complete fibroblast medium and cell numbers were counted using a haemocytometer on respective days. Means of three observations.

The growth curve assay showed that the growth of cells did not differ significantly during the first 2-3 days. However, from day 4 on, the growth rate of CD248_Δ sushi cells significantly increased relative to untransfected cells and CD248_Δ EGF cells (Figure 9). Therefore, the overexpression of CD248_Δ sushi appeared to increase the growth rate of MG63 cells.

3.3 Conclusions and Discussion

This chapter aimed to describe the generation and characterisation of CD248 mutants in an effort to determine which structural domains may be responsible for these known effects. Some of the technical issues identified while performing this work will now be discussed

The first step involved using an Overlapping extension PCR-based method in an effort to generate a variety of CD248 mutants whereby specific whole domains were deleted individually. Methods used for the fusion of two (or more) DNA fragments include conventional RE cloning and adaptors which is often tedious, time consuming and requires the introduction of unwanted sequences (Shevchuk et al. 2004). A quicker, more precise quicker alternative method is commonly known as overlap extension PCR. This method was used to successfully create precise deletion mutants with 100% sequence accuracy as evidenced by subsequent DNA sequencing of final plasmid DNA, but several technical points should be taken into consideration. First, it is important that the primers have very similar Tm values, which is vital for annealing and amplification within the final fusion PCR reaction (Kuwayama et al. 2002). Secondly, the third fusion PCR reaction should be performed with purified PCR products free from previous

primers, as these can inhibit the accuracy of such reaction. Once the mutant (and wildtype) CD248 genes were subcloned into the mammalian expression vector of choice, CD248-expressing stable MG63 cells were generated via a standard lipofectamine 2000 transfection method. The same technique has been done previously to generate WTCD248-expressing MG63 cells (Hardie et al. 2011), but never before with such mutants.

Immunofluorescence staining of stably-transfected cells indicated that the subcellular distribution of CD248 was not consistent across all transfected cell populations. The localisation of CD248 in CD248_Δ sushi, CD248_Δ EGF cell surface-expressing MG63 cells across the entire cell surface, whereas CD248 staining in CD248_WT, CD248_Δ CTLD, CD248_Δ mucin and CD248_Δ cytoplasmic stably-expressing cells was predominantly cytoplasmic, with very little cell surface expression. This observation of cell surface expression was confirmed during FACs analysis, by measuring the percentage of CD248 cell surface expressing cells within each population. This contradicts previous literature that CD248 is expressed predominantly at the cell surface *in vitro* (Rettig et al. 1992, Christian et al. 2001, Brady et al. 2004). But interestingly, this localization is similar to that seen for thrombomodulin following transfection, permeabilization and immunostaining of cultured cells (Teasdale et al. 1994). The cytoplasmic staining of CD248_WT, CD248_Δ CTLD, CD248_Δ mucin and CD248_Δ cytoplasmic stably-expressing cells could be explained by a number of possibilities. The most likely explanation is that the overexpression of exogenous CD248 or the myc tag at the c terminus may have caused aberrant accumulation of CD248 in intracellular secretory organelles. In terms of the mutants, the deleted sequence (ie. CTLD, mucin and

cytoplasmic tail) may be needed for transport from the ER and localization to the plasma membrane. Such intracellular expression may also represent an immature form as it is processed through the golgi, as previous literature has reported the presence of CD248 in recycling endosomes (Opavsky et al. 2001).

In order to find out which domains were important for growth rate characteristics, it was important to use cells that expressed CD248 on the cell surface. For this reason, growth curve analysis was only performed on the CD248_Δ sushi, CD248_Δ EGF cell surface-expressing MG63 cells. Growth curve analysis demonstrated that the overexpression of CD248_Δ sushi increased the growth rate of MG63 cells. This data matched previous findings within the lab that overexpression of wild-type CD248 increased the proliferation of MG63 cells (Hardie et al 2011). On the other hand, overexpression of CD248_Δ sushi did not increase the growth rate of such cells. This data suggests that the EGF repeat domain may be the key region of CD248 responsible for controlling the proliferation of MG63 cells, whereas the sushi domain is not.

However, it is important to be aware of the potential limitations of such techniques. Firstly, the MG63 cell type may not be the best model system for studying CD248 function, and fibroblasts and perciytes might represent a more physiologically relevant system. In addition, simple growth curve analysis may not be the best functional assay to study cell proliferation, and assays including thymidine incorporation and BrdU readout may represent more accurate experiments. For example, these are commonly performed over a range of cell densities, which is important as CD248 has been shown to be effected by cell density (Opavsky et al 2001).

CHAPTER 4

CRYSTALLISATION OF CD248

CHAPTER 4 – CRYSTALLISATION OF CD248

4.1 Introduction

The C-type lectin (CTL) superfamily is a well-studied group of metazoan proteins, both structurally and functionally. They have been shown to have diverse functions such as adhesion and glycoprotein synthesis. The Group XIV Thrombomodulin subgroup have also been well studied from a functional perspective, however, there is a distinct lack of knowledge concerning the 3 dimensional structure of type XIV proteins, with only the partial crystal structure of thrombomodulin having been resolved in complex with thrombin (Fuentes-Prior et al. 2000).

Numerous studies have reported the upregulation of CD248 and highlighted the role of CD248-expressing stromal cells within the tumour microenvironment and inflammatory microenvironment. Both scenarios are characterised by an activated stromal compartment and mesenchymal cell involvement. At the cellular level, CD248 has been linked to cellular effects including proliferation, adhesion and migration of stromal cells (Christian et al. 2008, Tomkowicz et al. 2007). Recent publications suggest that ectodomain interactions with extracellular matrix proteins may explain such functional effects (Tomkowicz et al. 2007).

Despite these studies, the structural and molecular basis of CD248 function is still unclear. Therefore, this chapter describes the recombinant expression of its entire

extracellular domain (as well as CTLD alone), purification and crystallisation of CD248, for future crystallographic analysis of the receptor.

4.2 Results

4.2.1 Production and crystallisation of CD248 c-type lectin domain (CTLD)

This section describes the production of soluble CD248 CTLD in quantities sufficient for use in x-ray crystallographic studies.

CD248 was originally expressed in *E.coli* BL21 (DE3) cells in the form of inclusion bodies (Figure 10), which were then purified and solubilized in 8M Urea buffer. The CD248CTLD-containing bacterial expression vector was previously generated in the lab (by Sarah Nichols, PEF facility). CTLD protein was expressed at a relatively high level and purity in the inclusion bodies, seen as a single protein band ~16 kDa on the SDS page gel (Figure 10A). The inclusion bodies were then subjected to standard chemical refolding methods (Methods section 2.2.2.1) and purified by gel filtration chromatography (into 20 mM MES and 50 mM NaCl) as a single peak on the elution profile (Figure 10B). Subsequent analysis of pooled elution peak fractions on an SDS page gel identified a higher single protein band of an incorrect size (~ 30 kDa) suggesting that the CTLD domain may not be susceptible to *in vitro* refolding techniques. Despite considerable efforts to produce soluble homogenous CD248 CTLD in a bacterial expression system, these attempts were largely unsuccessful as the yields acquired from this method were too low and judged inadequate for downstream structural studies.

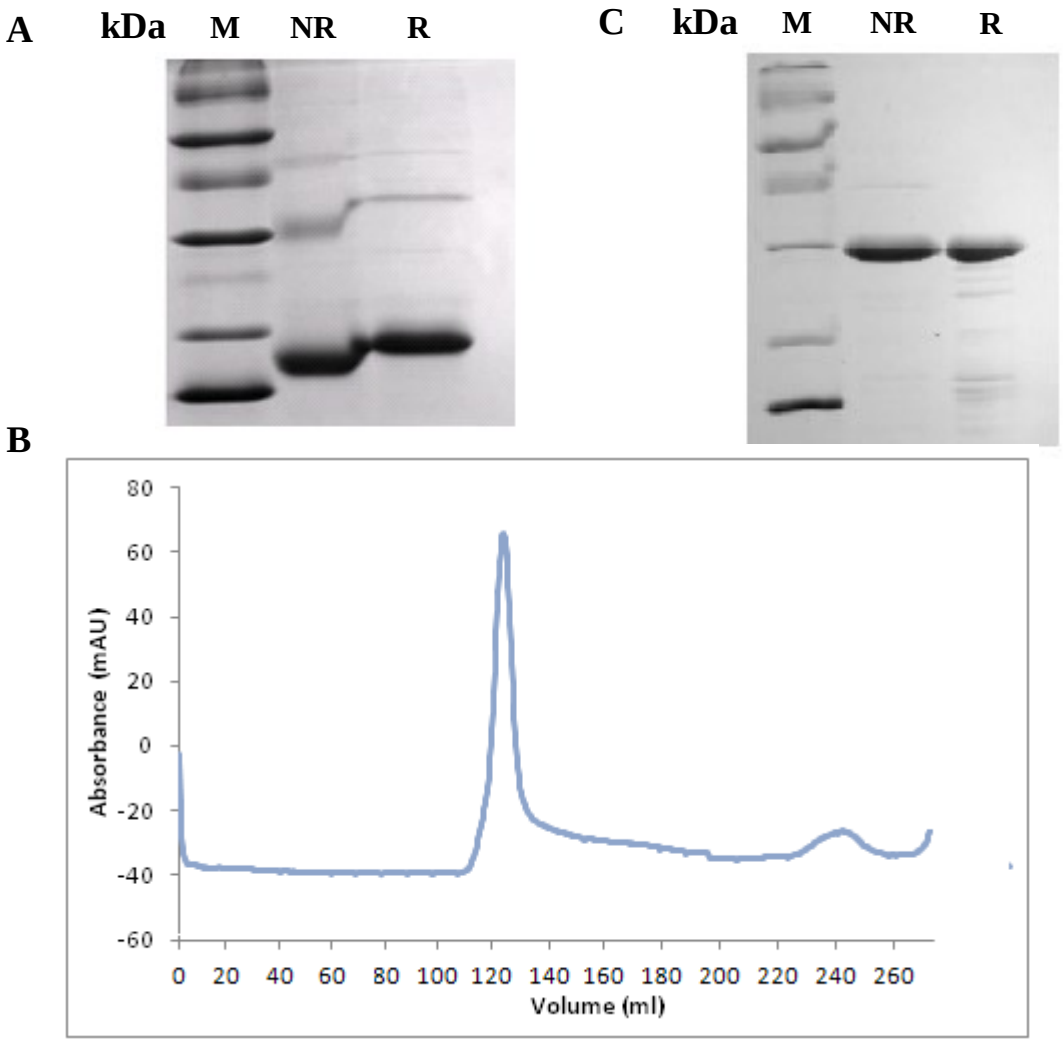

Figure 10. Expression, purification and SDS PAGE analysis of bacterially-expressed CD248 CTLD (**A**) SDS PAGE analysis of inclusion body preparation CD248 C-type lectin domain, under reducing and non-reducing conditions (**B**) size exclusion chromatography elution profile for CD248 CTLD after FPLC using S200 column. (**C**) SDS PAGE analysis of FPLC elution peak, under reducing and non-reducing conditions (predicted MW = 16 kDa).

Therefore, the CD248 CTLD was then expressed in an insect expression system using S2 cells as an alternative in an effort to produce soluble CD248 CTLD in quantities sufficient for use in structural studies. The CTLD expression construct was designed and generated by cloning the coding region of the gene into the pMT/BiP/V5-His expression vector, which was then used to transfect *Drosophila* S2 cells using calcium phosphate transfection method and create stable cell lines (Methods section 2.2.2.2) (Both conducted by Sarah Nichols, PEF facility). Transfection, expression and correct protein conformation were confirmed by western blotting the supernatant with an anti-His antibody (Figure 11A). The fact that CD248 CTLD was detected and displayed a shift in molecular weight between reducing and non-reducing conditions at 3-4 days post-transfection suggested correct protein conformation and disulphide bond pairing. The supernatant was then dialyzed into appropriate buffer prior to purification of his-tagged proteins by Ni-NTA chromatography (Methods section 2.2.2.5). Following NI-NTA chromatography, the purified and concentrated protein was analysed by SDS-PAGE (Figure 11B). It can be seen from Figure 11B, that the protein sample was of high purity, migrated at the expected size (~16 kDa) with very few contaminants following purification and obtained estimated yields of ~8-12 mg's/ Litre of supernatant. The *Drosophila* system produced higher yields of protein at required purity, adequate enough for crystallization purposes, without the need for further purification procedures. CTLD CD248 protein was purified into a standard Tris NaCl pH 8.0 buffer.

Drosophila-expressed protein was used to set up crystallisation trials. Initial CTLD crystallization screens were attempted at 5mg/ml, but unfortunately yielded no crystal hits and also experienced protein stability issues at concentrations greater than 5 mg/ml.

In order to obtain high enough protein concentrations for successful crystallization (ie. above 5 mg/ ml), an optimum buffer in which the protein is stable and soluble was required. For this reason, a thermal shift screening assay was conducted (with the help of Dr Timothy Knowles, Figure 12C). Buffer optimization involved choosing a buffer which increases the melting temperature (Tm) of your protein. It can be seen from Figure 12C and D that a number of different buffers produced a shift in melting temperature compared to the standard Tris Nacl buffer. For example, 50mM MES 100 mM $Cacl_2$ had melting temperatures of 65°C. CD248 CTLD protein was re-purified into 50 mM MES 100 mM $CalCl_2$ buffer due to the predicted calcium binding nature of CTLDs, which subsequently allowed crystallization trials to be set up at higher concentrations of 11.6 mg/ml. Initially the hanging drop technique yielded 13 potential crystal hits. However, 11 out of 13 of these turned out to be salt crystals after negative controls were performed, which left 2 conditions that were potentially yielding protein crystals (2 of which can be seen in Figure 15, B and C); Structure screen condition # 2.6 0.1M Nickel chloride hexahydrate, Tris pH 8.5, 1M Lithium Sulphate, and 0.01M Zinc sulphate heptahydrate, MES pH 6.5, 25% v/v PEG-MME 550.

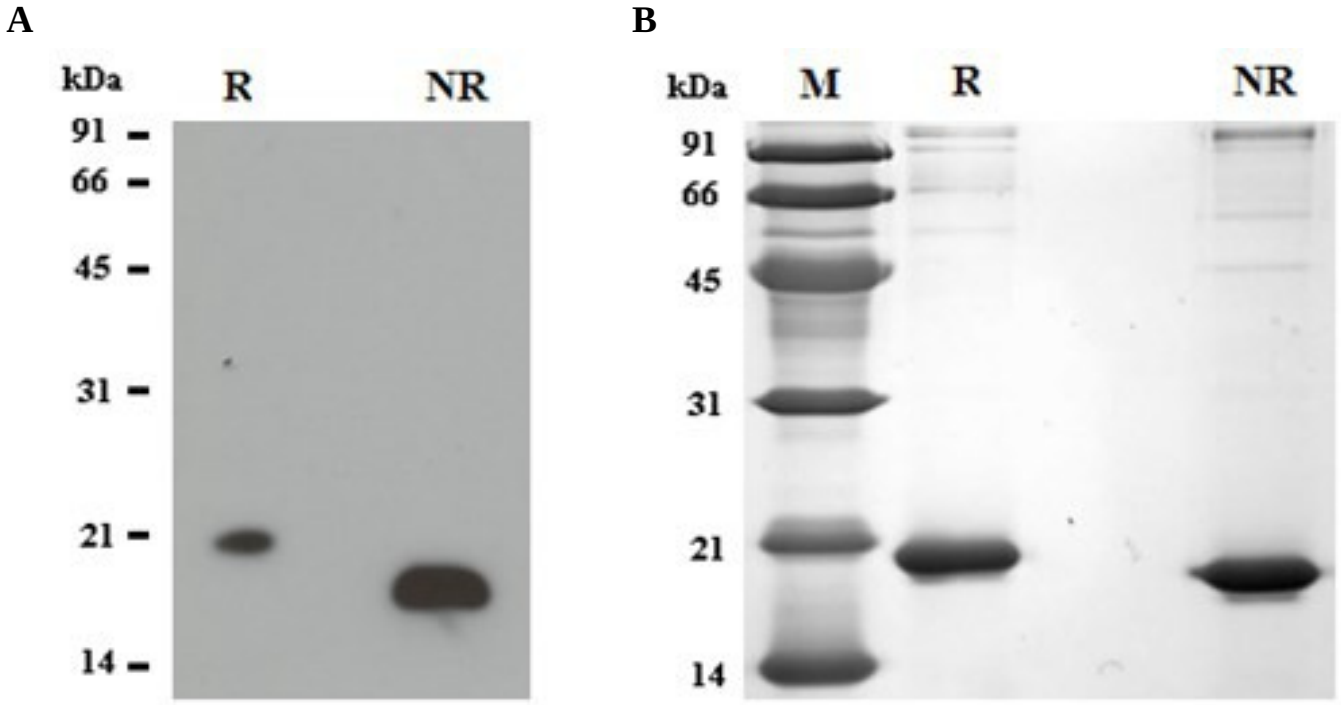

Figure 11. Expression, purification and SDS PAGE analysis of *Drosophila*-expressed CD248 CTLD (a): Western blot detection of CD248 CTLD expression under reducing and non-reducing conditions, at 72 h and 96 h post- induction, using anti-His antibody SDS PAGE analysis of CD248 CTLD overexpression in *Drosophila* S2 cells, under reducing and non-reducing conditions, (b): SDS-PAGE analysis of *Drosophila* derived CD248 CTLD following purification by Ni-NTA chromatography

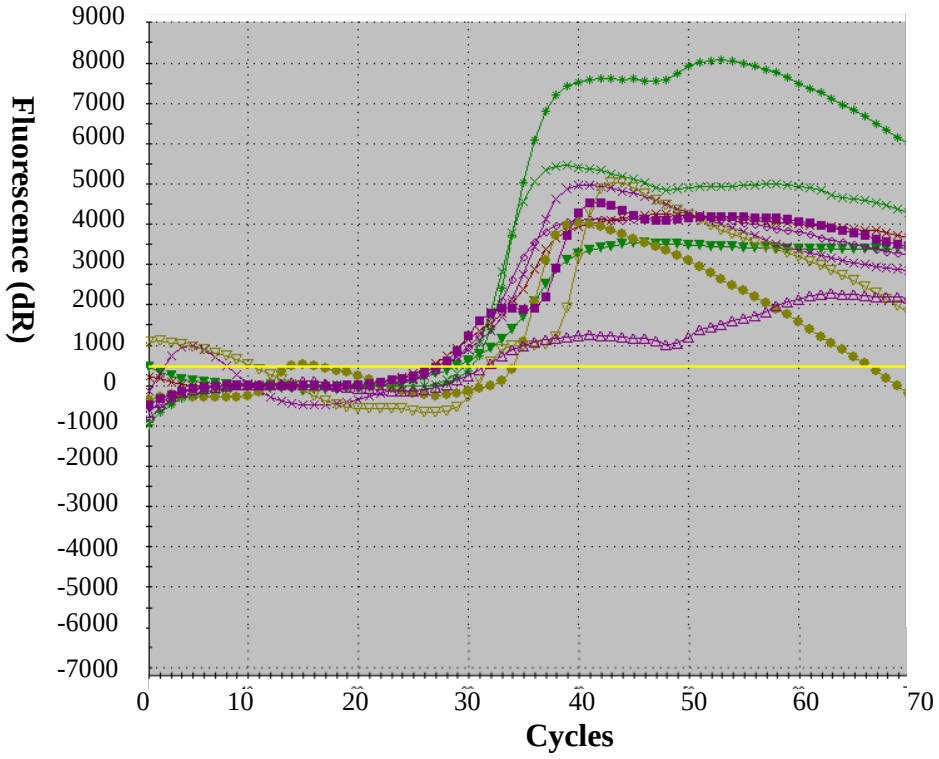

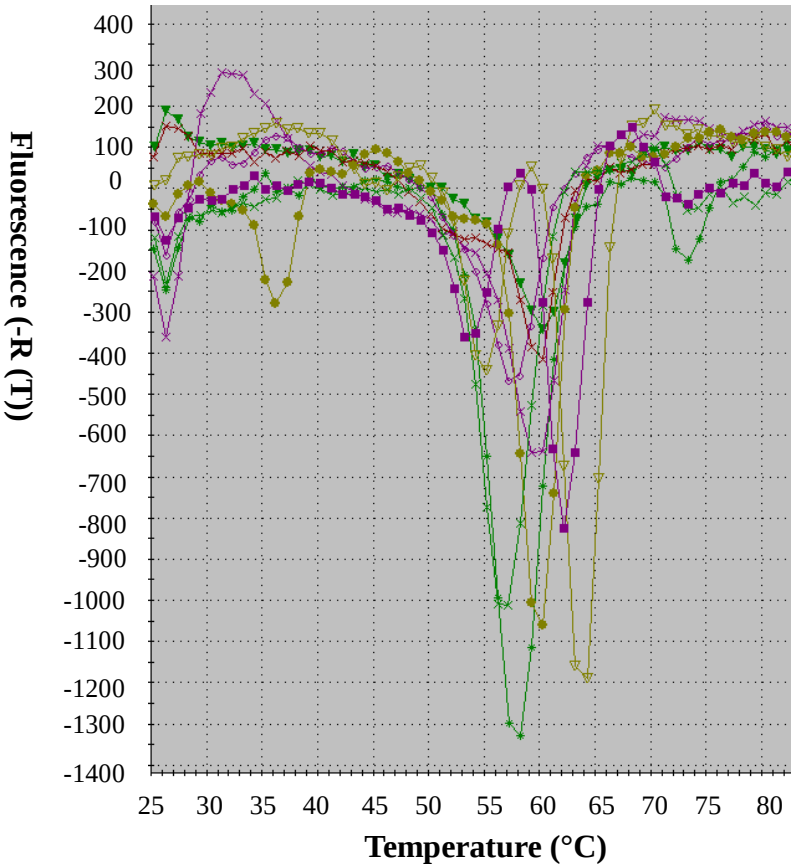

Symbol	Buffer	Additive	Tm (°C)	ΔTm (°C)
	MES	$CaCl^2$	65	15
	HEPES	NH^4Cl	62	12
	HEPES	$MgSO^4$	61	12
	Bis Tris	NaCl	60	10
	Bis Tris	$MgSO^4$	58	8
	Tris	NaCl	50	-

Figure 12. Thermafluor assay with CD248 CTLD. Melting curves and inverse melting temperatures (Tm) from thermafluor assay; both highlighting buffers that exhibited a significant change in thermal shift and Tm, compared to standard Tris NaCl buffer. Table highlighting corresponding optimum buffers.

4.2.2 Production and crystallisation of CD248 ectodomain.

This section describes the production of soluble CD248 ectodomain in quantities sufficient for use in x-ray crystallographic studies.

The CD248 ectodomain was expressed through the *Drosophila* system. Western blotting analysis revealed the induced expression of CD248 72 hours post induction in S2 stable cell lines (seen as a protein band ~38 kDa on western blot, Figure 13A). Following Ni-NTA chromatography, the purified protein product was then run on an SDS-PAGE gel which revealed successful purification of a band ~ 38 kDa corresponding to the full ectodomain, with a few high molecular weight residual contaminants (Figure 13B). In an effort to find an optimum buffer for purification, storage and crystallisation, a solubility assay was repeated for the full length version.

Protein was subjected to a further round of gel filtration chromatography using the S200 column in an effort to obtain higher purity for crystallization. The S200 elution profile shows that the protein eluted as a single peak ~220 mL (Figure 13C) SDS page analysis of this peak showed successful purification and purity greater than 95% that was suitable for crystallization attempts (Fig 13D).

The thermafluor assay highlighted a number of buffers that increased protein stability and solubility (Figure 14). The buffer formulation which greatly stabilized CD248 CTLD was 50 mM Bis-Tris, 150mM NaCl and 10% Glycerol (Tm 65°C), where the protein exhibited a 20°C increase in Tm in comparison with the initial storage and purification buffer (20 mM Tris, 50mM NaCl pH7.2).

Initial crystallization screens were set up following purification by gel filtration chromatography, at a relatively moderate concentration of 6 mg/ml in a hanging drop format. 1 out of 288 conditions yielded a potential protein hit in structure screen 1 condition # 19; 0.2M Zinc acetate, 0.1M Na cacodylate pH 6.5 and 18% w/v PEG-8K (Figure 15). Low rate of precipitation across many drops was evident which suggests a higher concentration of protein (10^{+} mg/ml) may yield more hits.

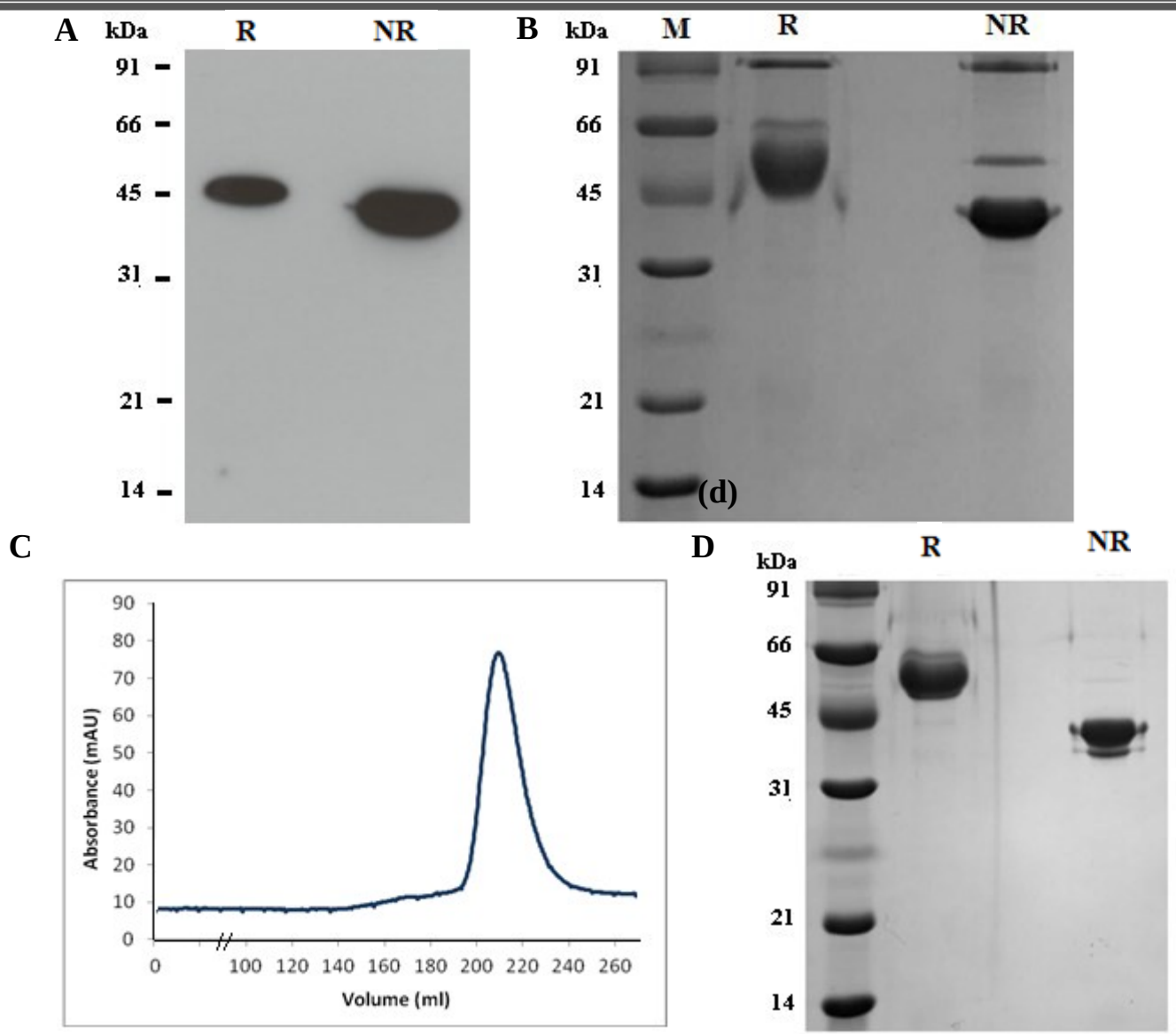

Figure 13. Expression, purification and SDS page analysis of CD248 ectodomain from a *Drosophila* S2 cell system. (**A**) Western blot detection of CD248 expression under reducing and non-reducing conditions, at 72 h and 96 h post- induction, using anti-His antibody. (**B**) SDS-PAGE analysis of *Drosophila* derived CD248 CTLD following purification by Ni-NTA chromatography. (**C**) size exclusion chromatography elution profile for full length CD248 CTLD post Ni-NTA purification using an S200 column. (**D**) SDS PAGE analysis of CD248 CTLD, following both Ni-NTA and SEC purification procedures.

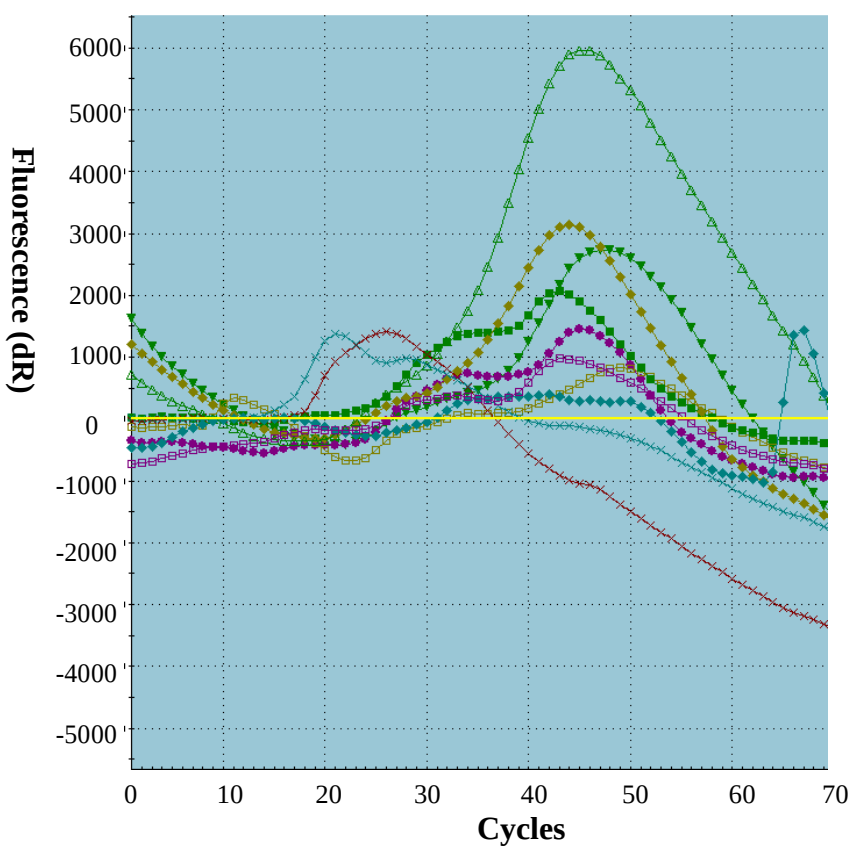

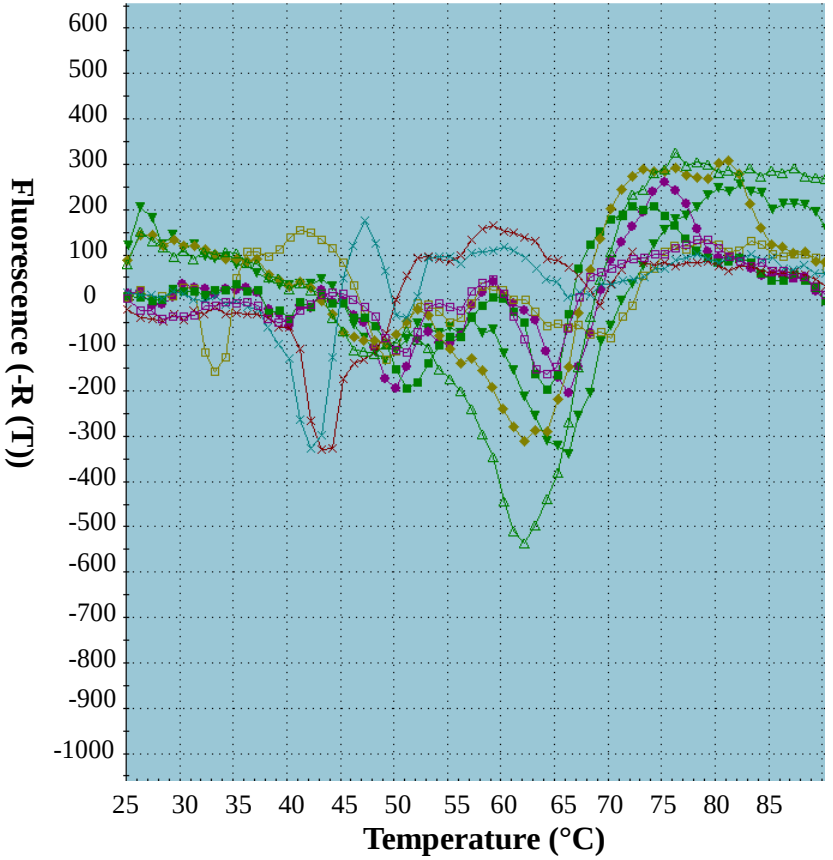

Symbol	Buffer	Additive(s)	Tm (°C)	ΔTm (°C)
	Bis Tris	NaCl, Glycerol (10%)	65	20
	Bis Tris	MgSO4	64	19
	Tris	MgSO4	63	18
	MES	$CaCl^2$	61	16
	Na cacodylate	NaCl, Glycerol (10%)	58	13
	Tris	NaCl	45	-

Figure 14. Thermafluor assay of CD248 ectodomain. Melting curves and inverse melting temperatures (Tm) from thermafluor assay; both highlighting buffers that exhibited a significant change in thermal shift and Tm, compared to standard Tris NaCl buffer. Table highlighting corresponding optimum buffers.

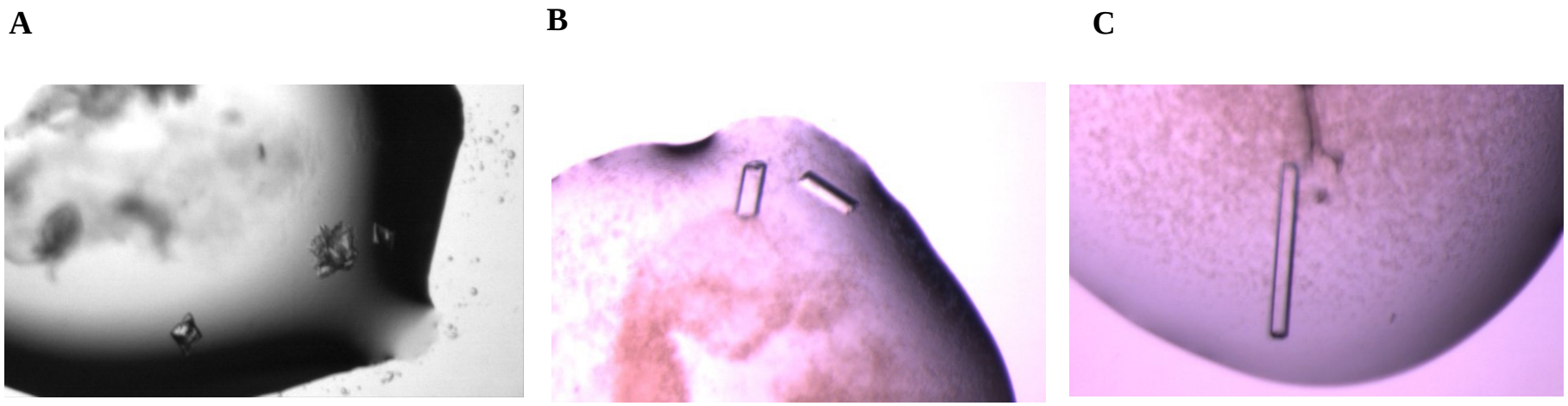

Figure 15. Initial protein crystal hits of CD248. (A) CD248 Ectodomain protein crystals obtained at 6 mg/ml in structure screen 1 condition # 19; 0.2M Zinc acetate, 0.1M NA cacodylate pH 6.5 and 18% w/v PEG-8K. (**B**) CD248 C type lectin domain protein crystals obtained at 11.6 mg/ml in Structure screen condition # 2.6 0.1M Nickel chloride hexahydrate, Tris pH 8.5, 1M Lithium Sulphate. (**C**) 0.01M Zinc sulphate heptahydrate, MES pH 6.5, 25% v/v PEG-MME 550.

4.3 Conclusions and Discussion

The aim of this chapter was to describe the production of soluble CD248 CTLD and entire ectodomain, in quantities sufficient for use in x-ray crystallographic studies. Some of the technical issues identified while performing this work will now be discussed.

The CTLD domain of wild type CD248 was originally produced using *E. coli* expression system and *in vitro* refolding methodologies. However, despite considerable efforts to produce soluble homogenous protein, these attempts were largely unsuccessful. Although protein was expressed to high levels in the inclusion bodies, the amount and identity of the refolded protein was incorrect and inadequate for crystallisation purposes. The fact that the protein was expressed at a high rate in the inclusion bodies indicates that it was the efficiency of the folding procedure that was the main barrier. In an effort to bypass the barrier of chemical refolding, the *Drosophila melanogaster* S2 expression system was used as an alternative and was found to be the more suitable expression system for CD248 CTLD protein production. Ni-NTA chromatography was used to purify resultant his-tagged proteins. This system was able to produce high yields of protein at the required purity, adequate enough for crystallisation screening. This was likely due to the efficient post translational modifications processes that take place in such cells.

Once high levels of purified, pure protein were successfully achieved, the next stage was then to set up crystallization trials in an attempt to find conditions that may yield protein crystals. One problem that became apparent was inherent protein stability issues,

in particular reduced solubility at higher protein concentrations. It is common knowledge within protein crystallography, that a protein must be homogenous, stable and soluble within its buffer for subsequent crystallization trials to be successful. The screening of protein buffers using thermal shift assays allowed the identification of buffers which increased the melting temperature and overall protein stability of CTLD protein in solution. *Drosophila*-expressed CD248 CTLD protein was used to set up crystallisation trials. The hanging drop method yielded 13 potential protein hits, whereas the sitting drop method yielded only 8 hits.

A thermofluor assay was used as an optimization buffer screen for the CD248 CTLD protein stability and solubility. The fact that calcium was required in the buffer for increased protein stability, solubility and crystal formation suggests that CD248 CTLD may require the binding of ionic calcium for protein stability and function. Another key issue during crystallization screening was the difficulty differentiating between salt and protein crystals within the drops. There are a few different ways of finding out whether protein hits are genuine by performing negative protein control plates as well as more sophisticated methods such as UV fluorescence protein detection systems. In my case, fluorescence protein detection was inconclusive due to practical reasons surrounding the plate dimensions, so the hits deemed as genuine protein crystals was based on negative protein control plates. Some of the hits produced on small scale are ready susceptible to enter optimization and or large scale methods to produce larger crystals adequate enough for x-ray diffraction

The ectodomain of CD248 protein was produced through the *Drosophila* S2 system. In order to obtain purity high enough for structural studies, the expressed protein required two rounds of purification by Ni-NTA then a further round of gel filtration chromatography using an S200 column. The screening of protein buffers was performed using thermal shift assays which allowed the identification of buffers that increased the melting temperature and overall protein stability of ectodomain protein in solution. The presence of calcium in the buffer appeared to increase the melting temperature and overall stability of CD248 ectodomain in solution, similar to its CTLD, which indicates that it may too have an ionic calcium binding function. This observation could perhaps be explained in terms of structural features. Both the CTLD and ectodomain contain cysteine residues and predicted disulphide bonds, therefore it is a possibility that the severe aggregation seen without calcium in the buffer is due to the formation of intermolecular disulphides, whereas the presence of calcium stabilizes such bonds.

Initial crystallisation screening of soluble ectodomain protein (5^{+} mg/ml) resulted in 1 potential protein hit. The fact that there was a low rate of precipitation across many of the drops suggested that a higher concentration of protein (10^{+} mg/ml) may yield more hits. The initial crystal hit was deemed not good enough for crystallographic analysis and require further optimisation and scale up. However, this work provides a good stepping stone for determining the x-ray crystallographic structure of CD248 in the future.

CHAPTER 5

CD248 SIGNALLING IN BONE FORMATION

CHAPTER 5 – CD248 SIGNALLING IN BONE FORMATION

5.1 Introduction

As mentioned earlier, CD248 also has a known role in inflammatory disorders. For example, (Smith et al. 2011) reported an upregulation of CD248-expressing stromal cells and direct association with known determinants of chronic kidney disease (CKD). In addition, another study demonstrated an upregulation of CD248-expressing stromal fibroblasts within the rheumatoid joint (MacFadyen et al. 2005). Inflammatory conditions such as rheumatoid arthritis are characterised by inflammatory-induced focal bone loss, which is thought to be due to aberrant osteogenesis. A number of studies have linked perturbed osteoblast function to such site-specific bone loss (Gravallese et al. 1998, Walsh et al. 2009). CD248 is a mesenchymal stem cell (MSC) marker (Bagley et al. 2009). MSCs are highly plastic in nature, and have the ability to differentiate into adipocytes (fat), chondrocytes (muscle) or osteoblasts (bone). In fact, *in silico* mining of gene expression data (Su et al. 2004) has shown that CD248 is highly expressed on osteoblasts.

The Rheumatology Research Group (RRG) has explored the role of CD248 in bone formation in CD248 deficient mice. The following observations have been reported; mice deficient in CD248 display increased bone mass, osteoblasts derived from such mice display an increased bone mineralisation capacity *in vitro*, due to an increase in osteoblast differentiation (Naylor et al. 2012).

However, the molecular mechanism by which CD248 causes such effects was unknown. Previous literature highlighting the involvement of CD248 in pericyte PDGFR signalling pathways, suggest a similar mechanism in osteoblast function.

In this chapter, we indeed provide evidence that the PDGF receptor and the MAP kinase ERK-1/2 may be involved in the CD248-regulated signalling pathways that control osteoblast function and subsequent bone formation.

5.2 Results

5.2.1 CD248 regulates PDGF-BB induced ERK phosphorylation in osteoblasts

Upon PDGFR phosphorylation, multiple intracellular signalling kinases are activated such as MAP kinase ERK1/2, leading to the upregulation of the transcription factor cFos (Tomkowicz et al. 2010). Therefore, to test whether PDGF signalling was perturbed in CD248-deficient mouse osteoblasts, we sought to determine the phosphorylation state of ERK1/2 at 0, 1 and 5 minutes post-induction with PDGF-BB.

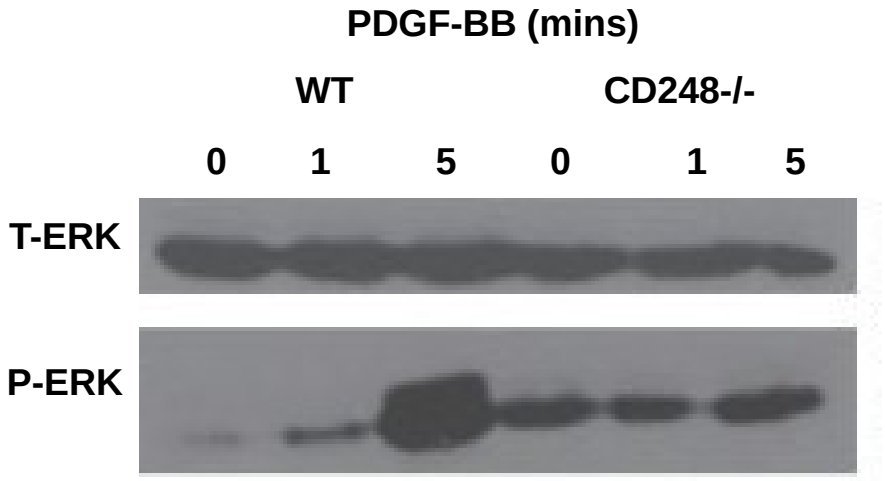

Figure 16. CD248 regulates PDGF-BB induced ERK phosphorylation in osteoblasts. Total ERK (t-ERK) and phosphorylated ERK (p-ERK) were assessed by Western blotting in osteoblasts from WT and CD248-/- mouse tibiae exposed to PDGF-BB for 0, 1, or 5 minutes.

It can be seen from Figure 16, that WT mouse osteoblasts displayed robust ERK-1/2 phosphorylation 5 minutes post-stimulation with PDGF-BB. However, mouse osteoblasts deficient in CD248 exhibited a reduced level of PDGF-BB-induced ERK-1/2 phosphorylation at the same time point. It is also important to note that the protein levels of total ERK (t-ERK) remained the same across different cells and time-points as expected.

5.3 Conclusions and Discussion

The aim of this chapter was to determine whether CD248 is required for PDGF signalling in osteoblasts, and in turn identify a possible molecular mechanism by which CD248 causes its effects on osteoblast differentiation and function.

Upon induction of osteoblasts with PDGF-BB, CD248 was shown to regulate the phosphorylation of the MAPK ERK-1/2. More specifically, the loss of CD248 expression was shown to disrupt downstream signals originating from the PDGF receptor on osteoblasts by reducing the activation of MAPK kinase ERK-1/2. These results match previous findings that CD248 is required for PDGF signalling in pericyte's (Tomkowicz et al. 2010).

Whenever performing western blotting for signalling analysis it is important to be aware of some of the inherent limitations surrounding this technique. Examples include problems concerning antibody specificity and suboptimal quantitation of protein levels. Therefore, additional methods have been used to investigate further and achieve reliable evidence in terms of signalling. The Rheumatology Research Group has confirmed previous findings that human osteoblasts express PDGFR alpha (Horner et al. 1996, Madden et al. 1975). In addition, osteoblasts from wild type mice were shown to exhibit 12-fold upregulation of cFos (a downstream target of PDGFR) following post PDFG-BB-stimulation, whereas CD248 deficient osteoblasts did not, using Real-time reverse transcription–polymerase chain reaction (RT-PCR) (Naylor et al. 2012).

These results together demonstrate that CD248 is required for PDGF signalling in osteoblasts, which opens up the possibility of the PDGF receptor and the MAP kinase ERK-1/2 being directly involved with the CD248-regulated signalling pathways that control osteoblast function and subsequent bone formation.

CHAPTER 6 OVERALL DISCUSSION

AND FUTURE DIRECTIONS

CHAPTER 6 – OVERALL DISCUSSION AND FUTURE DIRECTIONS

6.1 Overall Discussion

Endosialin (CD248) belongs to an emerging family of cell surface receptors strongly linked to cancer and inflammation. CD248 is expressed at high levels during embryogenesis, but is absent in normal adult tissue. Interestingly, its expression is dramatically upregulated in disease tissue, most notably on a wide range of tumours and within the arthritic joint. Functional studies have highlighted an active role in growth, metastasis and blood vessel formation. Such effects may relate to the cell-restricted nature of CD248 on mesenchymal cell types such as fibroblasts, pericyte's, osteoblasts and mesenchymal stem cells-themselves. Despite such knowledge, little is known about the molecular basis of CD248 function and is therefore a high priority in the field. The overall aim of this research was to determine the molecular basis of CD248 function. In order to achieve this: firstly, CD248 mutants were generated and analysed in growth curve assays to define key functional domains, and secondly, soluble CD248 protein was expressed, purified and screened for protein crystals. Finally, the role of the CD248 in the context of osteoblast function and subsequent bone formation was investigated. The implications relating to such work will now be discussed.

6.1.1 Functional characterisation of CD248

CD248 has a known role in tumour growth, metastasis, wound repair and inflammation. Recent evidence suggests that CD248 may cause these effects by increasing the proliferation and migration of CD248-expressing stromal cells (Lax et al. 2010). Structurally, CD248 is composed of several functional domains; the C-type lectin domain (CTLD), the Sushi domain (S) and three EGF repeats (EGF) followed by the mucin-like region (MUCIN), the transmembrane section (TM) and the short cytoplasmic tail (CYT), (Christian et al. 2001). From a ligand perspective, the multidomain architecture of the ectodomain suggests that it may have multiple protein partners and in fact *in vitro* studies suggest that the ectodomain of CD248 may interact with numerous extracellular matrix proteins including collagen 1, 4 and fibronectin (MacFadyen et al. 2005) as well as a tumour derived ligand Mac-2 BP, commonly linked to metastasis (Becker et al. 2008). However, it is not yet known which region of the protein is critical for such ligand binding and functional effects.

The results presented within this thesis indicate that the EGF repeat domain is important for the proliferation of CD248-expressing cells. One possibility is that a known or unknown ligand may bind directly to the EGF repeat domain of CD248 which may activate intracellular signals that result in proliferation effects, possibly through the PDGF signalling pathway via upregulation of c-fos. When investigating the domains responsible for certain functions it is important to take into consideration other related family members. Previous literature has reported similar findings in terms of EGF repeats domains being linked to proliferative phenotypes. For example, a study looking at the structure and function of a related Group XIV member thrombomodulin, reported

that the EGF repeats present in the ectodomain were responsible for the proliferation of Swiss 3T3 cells *in vitro* (Hamada et al. 1995). In addition, the EGF repeat domain of coagulation factor XII has also been shown to demonstrate growth-promoting phenotypes in Hep G2 cells (Schmeidler-Sapiro et al. 1991).

Despite the known ligand binding functions of sushi domains in other proteins, the results presented within this thesis indicate that the Sushi domain of CD248 is not important for the proliferation of MG63 cells. This supports the theory that the sushi domain of CD248 does not take part in ligand binding that affects the proliferation of CD248-expressing cells.

The multiple functions exhibited by CD248 likely reflect the multidomain architecture of the ectodomain, and it is increasingly likely that that the different domains mediate different functions. A good example is thrombomodulin which in addition to its EGF mitogen-promoting effects, has also been shown to play an important role in preventing leukocytes from binding to the endothelium, via a CTLD-mediated interaction (Conway et al. 2002). It is interesting also to note that the most recently discovered Group XIV family member, Clec14A, has a known role in angiogenesis as a tumour endothelial marker (TEM), more specifically functioning in migration, tube formation and endothelial cell-cell adhesion via a CTLD-mediated interaction (Rho et al. 2011), (Mura et al. 2012).

There is growing interest in CD248 not only as a clinical biomarker but as a therapeutic target, for which there is a growing need. The current state of knowledge suggests that

the interaction between CD248-expressing stromal cells and extracellular matrix components represents a good strategy by interfering with the stromal contribution to cancer and inflammatory disease. There is currently a drive in the area of designing novel therapies which aim to inhibit CD248 in the form of potent blocking antibodies and small molecule inhibitors. Previous CD248-targeted antibodies have been directed towards the CTLD of CD248 in an effort to inhibit the migratory capacity of CD248-expressing cells which are enjoying some success (Tomkowicz et al. 2007). However, the findings presented here suggest that the EGF repeat domain may be a good target in an attempt to inhibit the proliferation of CD248-expressing cells, at sites of cancer and inflammation.

6.1.2 Is Calcium required for CD248 protein stability and function?

CD248 belongs to Group XIV family of C-type lectin proteins, which is a large well studied group of metazoan proteins with diverse functions such as adhesion and glycoprotein synthesis. The family consists of three other-related proteins; thrombomodulin (TBM), complement receptor protein (CD93) (Drickamer and Fadden 2002), as well as the most recently discovered, C-type lectin domain family member 14A (Clec14A), (Mura et al. 2012). As the classification suggests, they are all characterised by a CTLD protruding from the cell surface in addition to a sushi domain, epidermal growth factor repeats (EGF) and highly glycosylated mucin-like region. However, in spite of the name and classification, the binding of ionic calcium binding to CD248 has not been demonstrated.

It has recently been highlighted that the key amino acids involved in coordinating ionic calcium binding are not conserved in CD248, thrombomodulin or CD93 (Valdez et al. 2012) suggesting that the Group XIV family members do not contain any functional c-type lectin activity (Valdez et al. 2012). However, the results presented within this thesis contradict such thinking and indicate that ionic calcium binding may be required for CD248 structure, stability and function.

The structural domains that are most likely to require calcium include the CTLD itself as well as the EGF-repeat domain. Interestingly upon sequence analysis, the EGF-repeat domain has a predicted calcium-binding function. It contains not only an EGF-like calcium binding conserved site, but also contains an EGF-type aspartate/asparagine hydroxylation site (EMBL-EBI database). In fact, the reported thrombomodulin-

thrombin interaction is thought to be mediated through the EGF-repeat domain in a Ca^{2+}-dependent manner (Sadler et al. 1993). In addition, homologous EGF-repeat domains contained within fibrulin-1 have been shown to be responsible for binding of fibronectin in a Ca^{2+}-dependent manner also (Tran et al. 1997).

In addition to the protein ligand binding, there is also a possibility that CD248 could bind to carbohydrates in a Ca^{2+}-dependent fashion also. Indeed, the CTLD of selectins have been shown to mediate Ca^{2+}-dependent binding of glycosylated receptors on heterotypic cells, leading to inflammation and tissue repair (Bischoff 1997).

The results presented in this thesis may have implications in drug design and targeted therapies. When designing receptor antagonists it is important to take into consideration the effects of additives. For example, it has been previously reported that the binding of monoclonal antibodies to thrombomodulin is Ca^{2+}-dependent, which was manifested by a conformational change in the EGF-repeat domain. More specifically it was shown that higher concentrations of Ca^{2+} ions resulted in higher rate of receptor binding (Kimura et al. 1989).

6.1.3 CD248: a therapeutic target in rheumatoid arthritis

During normal bone development, immature osteoblast cells are recruited to the site of bone formation (Maes et al. 2010) whereby they are known to play an active role in tissue remodelling and repair. More specifically, they are kept in an immature proliferative and pro-migratory state via PDGF signalling and ERK phosphorylation (Sanchez-Fernandez et al. 2008) . Another study has shown that the downstream target of PDGFR, c-fos (transcription factor) enhances cell cycle progression in osteoblasts, further highlighting the role of PDGFR signalling in osteoblast function (Sunters et al. 2004). Upon differentiation, mature osteoblasts modify their phenotype and become mostly non-proliferative and upregulate type 1 collagen (Liu et al. 1997). In certain inflammatory disorders such as RA this process is perturbed, and more specifically is characterised by inflammation-induced focal bone loss. Within the inflammatory microenvironment, osteoclast differentiation is enhanced and osteoblast-mediated bone formation is inhibited leading to bone erosion and overall net loss in weight. A number of studies have reported a lack of mature osteoblasts at the sites of focal bone erosion in RA (Gravallese et al. 1998) and murine inflammatory arthritis (Zwerina et al. 2006) and have linked perturbed osteoblast function to site-specific bone loss (Walsh et al. 2009).

The Rheumatology Research Group (RRG) has explored the role of CD248 in bone formation in CD248 deficient mice. The following observations have been reported; mice deficient in CD248 display increased bone mass, osteoblasts derived from such mice display an increased bone mineralisation capacity *in vitro*- due to an increase in osteoblast differentiation (Naylor et al. 2012). Previous literature highlighting the involvement of CD248 in pericyte PDGFR signalling pathways suggested a similar

mechanism in osteoblast function. The results reported within this thesis and from the group demonstrate that CD248 is required for PDGF signalling in mouse osteoblasts. Additional experiments performed within the lab have also shown that this CD248-PDGFR signalling interaction was vital for subsequent osteoblast proliferation and osteogenesis. Indeed, such studies have shown that the proliferation of PDGF stimulated CD248 -/- mouse osteoblasts is significantly reduced and produce more bone nodules compared to wild-type osteoblasts (Naylor et al. 2012).

Although the signalling mechanisms by which CD248 mediates its functions in the past have been controversial (Lax et al. 2010), the results within this thesis support previous literature from (Tomkowicz et al. 2010), where they showed that the PDGF-BB-dependant proliferation of pericyte's involved the PDGF receptor, subsequent phosphorylation of MAP kinase ERK-1/2 and upregulation of the downstream target c-fos. Despite this established link, the exact location at which CD248 intersects PDGF downstream signalling is still to be determined. It has been previously suggested that CD248 may interact directly with and recruit phosphatidylinositol 3 or Src-kinase's to amplify PDGF-BB-induced signals deriving from the PDGF receptor (Valdez et al. 2012). This hypothesis is supported by the results within this thesis, which highlight that the signalling defect is downstream of PDGFR, but upstream of ERK. The small cytoplasmic tail has no known kinase function but potential phosphorylation sites may interact with intracellular molecules in a direct or indirect-fashion.

Over the past few years, there has been an interest in targeting the PDGFR-B and associated signalling pathway as a useful approach in guided tissue regeneration. The

key disadvantage of targeting PDGFR-B is its widespread expression means that the functions of many cell types are likely to be affected if inhibited. However, CD248's restricted cell and tissue-specific expression profile at sites of inflammation and remodelling, in combination with the results from this thesis and data generated from the lab (Naylor et al. 2012) provide evidence that targeting CD248 instead may represent a superior approach to targeting tissue regeneration and repair in the context of inflammation-associated bone loss.

6.2 Concluding remarks and future directions

In conclusion, work undertaken in this thesis has established a potential role of CD248's EGF-repeat domain in the proliferation of CD248-expressing cells. In addition, information regarding the potential calcium-requirement of CD248 has also been provided which may aid further structural, ligand and functional studies. Finally, a molecular mechanism has been determined which explains the observed effect of CD248 in osteoblast function and bone formation, which in combination with other data suggests that CD248 may be a strong target for treating inflammation-associated bone loss in rheumatoid arthritis patients. Importantly, key reagents and assays have been developed which will underpin future studies when examining the structure and function of CD248.

An important next step in this field is to elucidate the structure of CD248, specifically its ectodomain. Establishing the three dimensional structure of CD248 is essential for gaining a comprehensive molecular understanding of CD248 function, and may allow the identification of potential ligand binding sites and possibly informing improved anti-

stroma therapeutic strategies by directing the design of inhibitors to block CD248 activity. Another important area of future work will include the identification of novel ligands and despite previous literature highlighting the binding of CD248 to extracellular matrix proteins, their precise mode of binding has not yet been determined. Therefore determining the molecular properties of such ligand interactions remains a key aim.

Despite results described within this work, the functional characterization of CD248 remains to be fully solved. A recent study by Maia et al. (2010) has shown that the cytoplasmic tail is required for arthritis progression in mice. Therefore, further studies could use mutagenesis techniques to examine the function of the cytoplasmic tail in order to identify putative intracellular binding partners and interactions.

In conclusion, the research described here and associated future research will not only improve the basic understanding of CD248 function, but also aid in the design of novel blocking inhibitors in the ability to inhibit the stromal contribution to cancer and inflammatory disorders.

REFERENCES

Bagley, R. G., Honma, N., Weber, W., Boutin, P., Rouleau, C., Shankara, S., Kataoka, S., Ishida, I., Roberts, B. L. and Teicher, B. A. (2008a) 'Endosialin/TEM 1/CD248 is a pericyte marker of embryonic and tumor neovascularization', *Microvasc Res,* 76(3), 180-8.

Bagley, R. G., Rouleau, C., St Martin, T., Boutin, P., Weber, W., Ruzek, M., Honma, N., Nacht, M., Shankara, S., Kataoka, S., Ishida, I., Roberts, B. L. and Teicher, B. A. (2008b) 'Human endothelial precursor cells express tumor endothelial marker 1/endosialin/CD248', *Mol Cancer Ther,* 7(8), 2536-46.

Bagley, R. G., Weber, W., Rouleau, C., Yao, M., Honma, N., Kataoka, S., Ishida, I., Roberts, B. L. and Teicher, B. A. (2009) 'Human mesenchymal stem cells from bone marrow express tumor endothelial and stromal markers', *Int J Oncol,* 34(3), 619-27.

Becker, R., Lenter, M. C., Vollkommer, T., Boos, A. M., Pfaff, D., Augustin, H. G. and Christian, S. (2008) 'Tumor stroma marker endosialin (Tem1) is a binding partner of metastasis-related protein Mac-2 BP/90K', *FASEB J,* 22(8), 3059-67.

Bergers, G., Song, S., Meyer-Morse, N., Bergsland, E. and Hanahan, D. (2003) 'Benefits of targeting both pericytes and endothelial cells in the tumor vasculature with kinase inhibitors', *Journal of Clinical Investigation,* 111(9), 1287-1295.

Bhowmick, N. A., Neilson, E. G. and Moses, H. L. (2004) 'Stromal fibroblasts in cancer initiation and progression', *Nature,* 432(7015), 332-7.

Bischoff, J. (1997) 'Cell adhesion and angiogenesis', *J Clin Invest,* 100(11 Suppl), S37-9.

Brady, J., Neal, J., Sadakar, N. and Gasque, P. (2004) 'Human endosialin (tumor endothelial marker 1) is abundantly expressed in highly malignant and invasive brain tumors', *J Neuropathol Exp Neurol,* 63(12), 1274-83.

Buckley, C. D., Amft, N., Bradfield, P. F., Pilling, D., Ross, E., Arenzana-Seisdedos, F., Amara, A., Curnow, S. J., Lord, J. M., Scheel-Toellner, D. and Salmon, M. (2000) 'Persistent induction of the chemokine receptor CXCR4 by TGF-beta 1 on synovial T cells contributes to their accumulation within the rheumatoid synovium', *J Immunol,* 165(6), 3423-3429.

Carson-Walter, E. B., Winans, B. N., Whiteman, M. C., Liu, Y., Jarvela, S., Haapasalo, H., Tyler, B. M., Huso, D. L., Johnson, M. D. and Walter, K. A.

(2009) 'Characterization of TEM1/endosialin in human and murine brain tumors', *BMC Cancer,* 9, 417.

Christian, S., Ahorn, H., Koehler, A., Eisenhaber, F., Rodi, H. P., Garin-Chesa, P., Park, J. E., Rettig, W. J. and Lenter, M. C. (2001) 'Molecular cloning and characterization of endosialin, a C-type lectin-like cell surface receptor of tumor endothelium', *J Biol Chem,* 276(10), 7408-14.

Christian, S., Winkler, R., Helfrich, I., Boos, A. M., Besemfelder, E., Schadendorf, D. and Augustin, H. G. (2008) 'Endosialin (Tem1) is a marker of tumor-associated myofibroblasts and tumor vessel-associated mural cells', *Am J Pathol,* 172(2), 486-94.

Conway, E. M., Van de Wouwer, M., Pollefeyt, S., Jurk, K., Van Aken, H., De Vriese, A., Weitz, J. I., Weiler, H., Hellings, P. W., Schaeffer, P., Herbert, J. M., Collen, D. and Theilmeier, G. (2002) 'The lectin-like domain of thrombomodulin confers protection from neutrophil-mediated tissue damage by suppressing adhesion molecule expression via nuclear factor kappaB and mitogen-activated protein kinase pathways', *J Exp Med,* 196(5), 565-77.

Dean, Y. D., McGreal, E. P., Akatsu, H. and Gasque, P. (2000) 'Molecular and cellular properties of the rat AA4 antigen, a C-type lectin-like receptor with structural homology to thrombomodulin', *J Biol Chem,* 275(44), 34382-92.

Demoulin, J. B. (2010) 'No PDGF receptor signal in pericytes without endosialin?', *Cancer Biol Ther,* 9(11), 916-8.

Drickamer, K. (1989) 'Multiple subfamilies of carbohydrate recognition domains in animal lectins', *Ciba Found Symp,* 145, 45-58, discussion 58-61.

Drickamer, K. (1999) 'C-type lectin-like domains', *Curr Opin Struct Biol,* 9(5), 585-90.

Drickamer, K. and Fadden, A. J. (2002) 'Genomic analysis of C-type lectins', *Biochem Soc Symp,* (69), 59-72.

Duroux-Richard, I., Jorgensen, C. and Apparailly, F. (2011) 'miRNAs and rheumatoid arthritis - promising novel biomarkers', *Swiss Med Wkly,* 141, w13175.

Franco, M., Roswall, P., Cortez, E., Hanahan, D. and Pietras, K. (2011) 'Pericytes promote endothelial cell survival through induction of autocrine VEGF-A signaling and Bcl-w expression', *Blood,* 118(10), 2906-17.

Fuentes-Prior, P., Iwanaga, Y., Huber, R., Pagila, R., Rumennik, G., Seto, M., Morser, J., Light, D. R. and Bode, W. (2000) 'Structural basis for the

anticoagulant activity of the thrombin-thrombomodulin complex', *Nature,* 404(6777), 518-25.

Gabbiani, G., Ryan, G. B. and Majne, G. (1971) 'Presence of modified fibroblasts in granulation tissue and their possible role in wound contraction', *Experientia,* 27(5), 549-50.

Garboczi, D. N., Hung, D. T. and Wiley, D. C. (1992) 'HLA-A2-peptide complexes: refolding and crystallization of molecules expressed in Escherichia coli and complexed with single antigenic peptides', *Proc Natl Acad Sci U S A,* 89(8), 3429-33.

Gravallese, E. M., Harada, Y., Wang, J. T., Gorn, A. H., Thornhill, T. S. and Goldring, S. R. (1998) 'Identification of cell types responsible for bone resorption in rheumatoid arthritis and juvenile rheumatoid arthritis', *Am J Pathol,* 152(4), 943-51.

Hamada, H., Ishii, H., Sakyo, K., Horie, S., Nishiki, K. and Kazama, M. (1995) 'The epidermal growth factor-like domain of recombinant human thrombomodulin exhibits mitogenic activity for Swiss 3T3 cells', *Blood,* 86(1), 225-33.

Hanly, A. M., Hayanga, A., Winter, D. C. and Bouchier-Hayes, D. J. (2005) 'Thrombomodulin: tumour biology and prognostic implications', *Ejso,* 31(3), 217-220.

Hardie, D. L., Baldwin, M. J., Naylor, A., Haworth, O. J., Hou, T. Z., Lax, S., Curnow, S. J., Willcox, N., MacFadyen, J., Isacke, C. M. and Buckley, C. D. (2011) 'The stromal cell antigen CD248 (endosialin) is expressed on naive CD8+ human T cells and regulates proliferation', *Immunology,* 133(3), 288-95.

Horner, A., Bord, S., Kemp, P., Grainger, D. and Compston, J. E. (1996) 'Distribution of platelet-derived growth factor (PDGF) A chain mRNA, protein, and PDGF-alpha receptor in rapidly forming human bone', *Bone,* 19(4), 353-62.

Huber, M. A., Kraut, N., Schweifer, N., Dolznig, H., Peter, R. U., Schubert, R. D., Scharffetter-Kochanek, K., Pehamberger, H. and Garin-Chesa, P. (2006) 'Expression of stromal cell markers in distinct compartments of human skin cancers', *J Cutan Pathol,* 33(2), 145-55.

Kalluri, R. and Zeisberg, M. (2006) 'Fibroblasts in cancer', *Nature Reviews Cancer,* 6(5), 392-401.

Kimura, S., Nagoya, T. and Aoki, N. (1989) 'Monoclonal antibodies to human thrombomodulin whose binding is calcium dependent', *J Biochem,* 105(3), 478-83.

Kuwayama, H., Obara, S., Morio, T., Katoh, M., Urushihara, H. and Tanaka, Y. (2002) 'PCR-mediated generation of a gene disruption construct without the use of DNA ligase and plasmid vectors', ***Nucleic Acids Research,*** **30(2).**

Lax, S., Hardie, D. L., Wilson, A., Douglas, M. R., Anderson, G., Huso, D., Isacke, C. M. and Buckley, C. D. (2010) 'The pericyte and stromal cell marker CD248 (endosialin) is required for efficient lymph node expansion', ***Eur J Immunol,*** **40(7), 1884-9.**

Lax, S., Hou, T. Z., Jenkinson, E., Salmon, M., MacFadyen, J. R., Isacke, C. M., Anderson, G., Cunningham, A. F. and Buckley, C. D. (2007) 'CD248/Endosialin is dynamically expressed on a subset of stromal cells during lymphoid tissue development, splenic remodeling and repair', ***FEBS Lett,*** **581(18), 3550-6.**

Liu, F., Malaval, L. and Aubin, J. E. (1997) 'The mature osteoblast phenotype is characterized by extensive plasticity', ***Experimental Cell Research,*** **232(1), 97-105.**

MacFadyen, J. R., Haworth, O., Roberston, D., Hardie, D., Webster, M. T., Morris, H. R., Panico, M., Sutton-Smith, M., Dell, A., van der Geer, P., Wienke, D., Buckley, C. D. and Isacke, C. M. (2005) 'Endosialin (TEM1, CD248) is a marker of stromal fibroblasts and is not selectively expressed on tumour endothelium', ***FEBS Lett,*** **579(12), 2569-75.**

Madden, J. W., Carlson, E. C. and Hines, J. (1975) 'Presence of modified fibroblasts in ischemic contracture of the intrinsic musculature of the hand', ***Surg Gynecol Obstet,*** **140(4), 509-16.**

Maes, C., Kobayashi, T., Selig, M. K., Torrekens, S., Roth, S. I., Mackem, S., Carmeliet, G. and Kronenberg, H. M. (2010) 'Osteoblast Precursors, but Not Mature Osteoblasts, Move into Developing and Fractured Bones along with Invading Blood Vessels', ***Developmental Cell,*** **19(2), 329-344.**

Maia, M., de Vriese, A., Janssens, T., Moons, M., van Landuyt, K., Tavernier, J., Lories, R. J. and Conway, E. M. (2010) 'CD248 and its cytoplasmic domain: a therapeutic target for arthritis', ***Arthritis Rheum,*** **62(12), 3595-606.**

Maia, M., DeVriese, A., Janssens, T., Moons, M., Lories, R. J., Tavernier, J. and Conway, E. M. (2011) 'CD248 facilitates tumor growth via its cytoplasmic domain', ***BMC Cancer,*** **11, 162.**

McGreal, E. and Gasque, P. (2002) 'Structure-function studies of the receptors for complement C1q', ***Biochemical Society Transactions,*** **30, 1010-1014.**

Mura, M., Swain, R. K., Zhuang, X., Vorschmitt, H., Reynolds, G., Durant, S., Beesley, J. F., Herbert, J. M., Sheldon, H., Andre, M., Sanderson, S., Glen,

K., Luu, N. T., McGettrick, H. M., Antczak, P., Falciani, F., Nash, G. B., Nagy, Z. S. and Bicknell, R. (2012) 'Identification and angiogenic role of the novel tumor endothelial marker CLEC14A', ***Oncogene,*** **31(3), 293-305.**

Nanda, A., Karim, B., Peng, Z. S., Liu, G. S., Qiu, W. P., Gan, C., Vogelstein, B., St Croix, B., Kinzler, K. W. and Huso, D. L. (2006) 'Tumor endothelial marker 1 (Tem1) functions in the growth and progression of abdominal tumors', ***Proc Natl Acad Sci U S A,*** **103(9), 3351-3356.**

Nangaku, M. (1998) 'Complement regulatory proteins in glomerular diseases', ***Kidney Int,*** **54(5), 1419-1428.**

Naylor, A. J., Azzam, E., Smith, S., Croft, A., Poyser, C., Duffield, J. S., Huso, D. L., Gay, S., Ospelt, C., Cooper, M. S., Isacke, C., Goodyear, S. R., Rogers, M. J. and Buckley, C. D. (2012) 'The mesenchymal stem cell marker CD248 (endosialin) is a negative regulator of bone formation in mice', ***Arthritis Rheum,*** **64(10), 3334-43.**

Nepomuceno, R. R., Ruiz, S., Park, M. and Tenner, A. J. (1999) 'C1qRP is a heavily O-glycosylated cell surface protein involved in the regulation of phagocytic activity', ***J Immunol,*** **162(6), 3583-9.**

Ohradanova, A., Gradin, K., Barathova, M., Zatovicova, M., Holotnakova, T., Kopacek, J., Parkkila, S., Poellinger, L., Pastorekova, S. and Pastorek, J. (2008) 'Hypoxia upregulates expression of human endosialin gene via hypoxia-inducible factor 2', ***Br J Cancer,*** **99(8), 1348-56.**

Opavsky, R., Haviernik, P., Jurkovicova, D., Garin, M. T., Copeland, N. G., Gilbert, D. J., Jenkins, N. A., Bies, J., Garfield, S., Pastorekova, S., Oue, A. and Wolff, L. (2001) 'Molecular characterization of the mouse Tem1/endosialin gene regulated by cell density in vitro and expressed in normal tissues in vivo', ***J Biol Chem,*** **276(42), 38795-807.**

Pietras, K. and Ostman, A. (2010) 'Hallmarks of cancer: interactions with the tumor stroma', ***Experimental Cell Research,*** **316(8), 1324-31.**

Pilling, D., Akbar, A. N., Girdlestone, J., Orteu, C. H., Borthwick, N. J., Amft, N., Scheel-Toellner, D., Buckley, C. D. and Salmon, M. (1999) 'Interferon-beta mediates stromal cell rescue of T cells from apoptosis', ***Eur J Immunol,*** **29(3), 1041-1050.**

Rettig, W. J., Garin-Chesa, P., Healey, J. H., Su, S. L., Jaffe, E. A. and Old, L. J. (1992) 'Identification of endosialin, a cell surface glycoprotein of vascular endothelial cells in human cancer', ***Proc Natl Acad Sci U S A,*** **89(22), 10832-6.**

Rho, S. S., Choi, H. J., Min, J. K., Lee, H. W., Park, H., Kim, Y. M. and Kwon, Y. G. (2011) 'Clec14a is specifically expressed in endothelial cells and mediates cell to cell adhesion', ***Biochem Biophys Res Commun,*** **404(1), 103-8.**

Rupp, C., Dolznig, H., Puri, C., Schweifer, N., Sommergruber, W., Kraut, N., Rettig, W. J., Kerjaschki, D. and Garin-Chesa, P. (2006) 'Laser capture microdissection of epithelial cancers guided by antibodies against fibroblast activation protein and endosialin', ***Diagn Mol Pathol,*** **15(1), 35-42.**

Sadler, J. E., Lentz, S. R., Sheehan, J. P., Tsiang, M. and Wu, Q. Y. (1993) 'Structure-Function-Relationships of the Thrombin-Thrombomodulin Interaction', ***Haemostasis,*** **23, 183-193.**

Sanchez-Fernandez, M. A., Gallois, A., Riedl, T., Jurdic, P. and Hoflack, B. (2008) 'Osteoclasts control osteoblast chemotaxis via PDGF-BB/PDGF receptor beta signaling', ***PLoS One,*** **3(10), e3537.**

Schmeidler-Sapiro, K. T., Ratnoff, O. D. and Gordon, E. M. (1991) 'Mitogenic effects of coagulation factor XII and factor XIIa on HepG2 cells', ***Proc Natl Acad Sci U S A,*** **88(10), 4382-5.**

Shevchuk, N. A., Bryksin, A. V., Nusinovich, Y. A., Cabello, F. C., Sutherland, M. and Ladisch, S. (2004) 'Construction of long DNA molecules using long PCR-based fusion of several fragments simultaneously', ***Nucleic Acids Research,*** **32(2).**

Simonavicius, N., Ashenden, M., van Weverwijk, A., Lax, S., Huso, D. L., Buckley, C. D., Huijber, I. J., Yarwood, H. and Isacke, C. M. (2012) 'Pericytes promote selective vessel regression to regulate vascular patterning', ***Blood,*** **120(7), 1516-27.**

Smith, S. W., Eardley, K. S., Croft, A. P., Nwosu, J., Howie, A. J., Cockwell, P., Isacke, C. M., Buckley, C. D. and Savage, C. O. (2011) 'CD248+ stromal cells are associated with progressive chronic kidney disease', ***Kidney Int,*** **80(2), 199-207.**

St Croix, B., Rago, C., Velculescu, V., Traverso, G., Romans, K. E., Montgomery, E., Lal, A., Riggins, G. J., Lengauer, C., Vogelstein, B. and Kinzler, K. W. (2000) 'Genes expressed in human tumor endothelium', ***Science,*** **289(5482), 1197-202.**

Su, A. I., Wiltshire, T., Batalov, S., Lapp, H., Ching, K. A., Block, D., Zhang, J., Soden, R., Hayakawa, M., Kreiman, G., Cooke, M. P., Walker, J. R. and Hogenesch, J. B. (2004) 'A gene atlas of the mouse and human protein-encoding transcriptomes', ***Proc Natl Acad Sci U S A,*** **101(16), 6062-6067.**

Sunters, A., Thomas, D. P., Yeudall, W. A. and Grigoriadis, A. E. (2004) 'Accelerated cell cycle progression in osteoblasts overexpressing the c-fos

proto-oncogene: induction of cyclin A and enhanced CDK2 activity', *J Biol Chem*, 279(11), 9882-91.

Szekanecz, Z., Besenyei, T., Szentpetery, A. and Koch, A. E. (2010) 'Angiogenesis and vasculogenesis in rheumatoid arthritis', *Current Opinion in Rheumatology*, 22(3), 299-306.

Teasdale, M. S., Bird, C. H. and Bird, P. (1994) 'Internalization of the Anticoagulant Thrombomodulin Is Constitutive and Does Not Require a Signal in the Cytoplasmic Domain', *Immunology and Cell Biology*, 72(6), 480-488.

Tomkowicz, B., Rybinski, K., Foley, B., Ebel, W., Kline, B., Routhier, E., Sass, P., Nicolaides, N. C., Grasso, L. and Zhou, Y. (2007) 'Interaction of endosialin/TEM1 with extracellular matrix proteins mediates cell adhesion and migration', *Proc Natl Acad Sci U S A*, 104(46), 17965-70.

Tomkowicz, B., Rybinski, K., Sebeck, D., Sass, P., Nicolaides, N. C., Grasso, L. and Zhou, Y. (2010) 'Endosialin/TEM-1/CD248 regulates pericyte proliferation through PDGF receptor signaling', *Cancer Biol Ther*, 9(11), 908-15.

Tran, H., VanDusen, W. J. and Argraves, W. S. (1997) 'The self-association and fibronectin-binding sites of fibulin-1 map to calcium-binding epidermal growth factor-like domains', *J Biol Chem*, 272(36), 22600-6.

Valdez, Y., Maia, M. and Conway, E. M. (2012) 'CD248: reviewing its role in health and disease', *Curr Drug Targets*, 13(3), 432-9.

Walsh, N. C., Reinwald, S., Manning, C. A., Condon, K. W., Iwata, K., Burr, D. B. and Gravallese, E. M. (2009) 'Osteoblast Function Is Compromised at Sites of Focal Bone Erosion in Inflammatory Arthritis', *Journal of Bone and Mineral Research*, 24(9), 1572-1585.

Weiler, H. and Isermann, B. H. (2003) 'Thrombomodulin', *Journal of Thrombosis and Haemostasis*, 1(7), 1515-1524.

Yoo, S. A., Kwok, S. K. and Kim, W. U. (2008) 'Proinflammatory role of vascular endothelial growth factor in the pathogenesis of rheumatoid arthritis: prospects for therapeutic intervention', *Mediators Inflamm*, 2008, 129873.

Zwerina, J., Tuerk, B., Redlich, K., Smolen, J. S. and Schett, G. (2006) 'Imbalance of local bone metabolism in inflammatory arthritis and its reversal upon tumor necrosis factor blockade: direct analysis of bone turnover in murine arthritis', *Arthritis Res Ther*, 8(1), R22.

APPENDIX

The following paper was published during the course of this project.

Naylor, A. J., Azzam, E., Smith, S., Croft, A., Poyser, C., Duffield, J. S., Huso, D. L., Gay, S., Ospelt, C., Cooper, M. S., Isacke, C., Goodyear, S. R., Rogers, M. J. and Buckley, C. D. (2012) 'The mesenchymal stem cell marker CD248 (endosialin) is a negative regulator of bone formation in mice', *Arthritis Rheum*, 64(10), 3334-43.

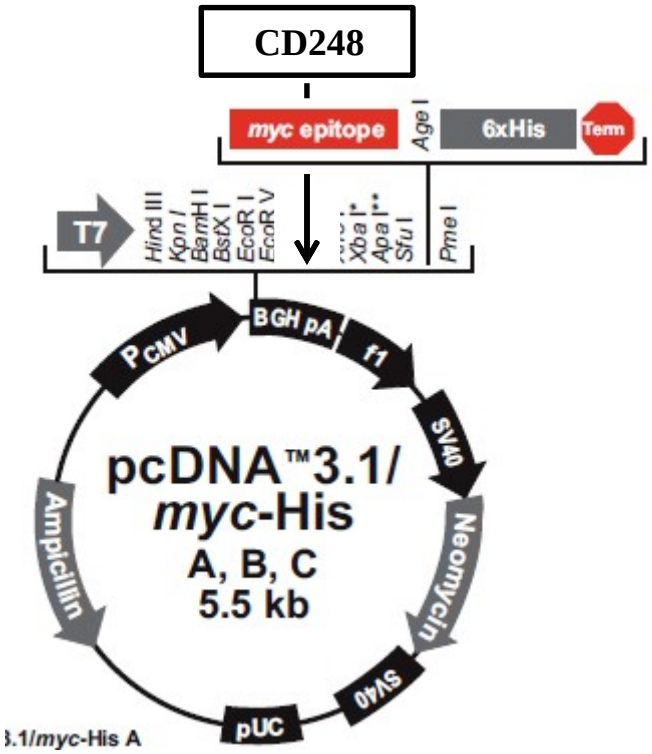

Map of pcDNA 3.1 myc his vector, with multiple cloning site (MCS) expanded to show restriction sites, CD248 donar site and features such as CMV promotor and neomycin restistance.